Planetary and Space Science 167 (2019) 54–70

Contents lists available at ScienceDirect

Planetary and Space Science

journal homepage: www.elsevier.com/locate/pss

Constraints on the nature of the effusive volcanic eruptions that incised Ravi Vallis, Mars

David W. Leverington

Department of Geosciences, Texas Tech University, Lubbock, TX, 79409, USA

ARTICLE INFO

Keywords:
Mars
Channel
Volcanism
Lava

ABSTRACT

Ravi Vallis is a Martian outflow channel that is widely interpreted as a product of one or more catastrophic outbursts of groundwater from adjacent Aromatum Chaos. However, solar system analogs are unknown for formation of large channels by outbursts from aquifers, and the Ravi Vallis region lacks the obvious sedimentological and mineralogical signatures expected of aqueous origins. Instead, the basic nature of this channel system is consistent with volcanic origins involving voluminous effusions of low-viscosity lavas. On bedrock slopes of only 0.2°, 50-m-deep lava flows with viscosities of 1 Pa s are predicted to have been characterized by discharge rates of $\sim 3 \times 10^7$ m^3/s for 25-km-wide flows, with associated mechanical incision rates of ~4 m/day and thermal incision rates of ~2 m/day. Formation of Aromatum Chaos and the preserved 215-km-long extent of Ravi Vallis is conservatively estimated on the basis of thermal considerations to have required eruption of a minimum of ~64,000 km^3 of lava, but greater volumes would have been necessary to form the original (unknown) length of this channel system. A volcanic origin for Ravi Vallis is consistent with development of all Martian outflow channels by igneous processes, and with the broader premise that early development of immense volcanic channel systems is typical of all large rocky bodies.

1. Introduction

The outflow channels of Mars consist of relatively large and low-order channel systems that commence either at ridged volcanic plains or, more typically, at topographic depressions that mark the sites of voluminous fluid effusions from the subsurface (e.g., Greeley et al., 1977; Baker, 1982; Mars Channel Working Group, 1983; Carr, 1996). The presence of anastomosing reaches, streamlined erosional residuals, cataracts, and other scabland features at these systems is reminiscent of terrestrial floodways such as those of the Channeled Scabland of Washington (e.g., Milton, 1973; Baker and Milton, 1974; Carr, 1974; Masursky et al., 1977). Partly on this basis, Martian outflow channels are widely interpreted as the products of catastrophic outbursts of groundwater from aquifers confined by frozen ground (e.g., Carr, 1979; Clifford, 1993, 2017; Clifford and Parker, 2001; Carr and Head, 2010, 2019; Rodriguez et al., 2012; Larsen and Lamb, 2016; Lapotre et al., 2016; Head et al., 2018; Baker, 2018; Zuber, 2018), though other mechanisms of formation such as those involving surface or near-surface interactions between ice and volcanic flows have also been proposed for some systems (e.g., Head et al., 2003; Cassanelli and Head, 2016, 2018a, b; Hamilton et al., 2018; Voelker et al., 2018). Aqueous interpretations of the Martian outflow channels have influenced estimates of near-surface volatile abundances (e.g., Squyres, 1989; Carr, 1996; Clifford and Parker, 2001; Carr and Head, 2015, 2019; Head et al., 2018; Baker, 2018), inferences regarding past variations in global climate (e.g., Sagan et al., 1973; Sharp and Malin, 1975; Toon et al., 1980; Baker, 2001, 2018), and hypotheses regarding the past capacity of the Martian environment to develop, support, and distribute life (e.g., McKay, 1992; Dohm et al., 2004; Levy and Head, 2005; Schulze-Makuch et al., 2007; Warner et al., 2010; Durrant et al., 2017; Cabrol, 2018).

Ravi Vallis is a relatively small Hesperian-aged outflow channel that is located in the highlands of Xanthe Terra, between Shalbatana Vallis and Hydraotes Chaos (e.g., Carr, 1979, 2012; Komar, 1979; Nummedal and Prior, 1981; Mars Channel Working Group, 1983; Moore et al., 1995; Nelson and Greeley, 1999; Max and Clifford, 2001; Coleman, 2003; Coleman and Baker, 2009; Mangold et al., 2016) (Fig. 1). The absence of tributary channels at Ravi Vallis suggests its incision by fluids expelled from the subsurface at adjacent Aromatum Chaos, and this system is predominantly interpreted as a product of one or more catastrophic outbursts of groundwater here (e.g., Moore et al., 1995; Nelson and Greeley, 1999; Coleman, 2005; Marra et al., 2014; Berman et al., 2018). However, proposed aqueous origins for Ravi Vallis and other Martian

E-mail address: david.leverington@ttu.edu.

https://doi.org/10.1016/j.pss.2019.01.002
Received 27 July 2018; Received in revised form 3 January 2019; Accepted 4 January 2019
Available online 7 January 2019

outflow channels suffer from problematic issues including the implausibility of involved processes, a lack of relevant analogs, incongruities between aqueous hypotheses of channel formation and surface mineralogy, and the absence of sedimentary deposits of obvious fluvial or diluvial origin along component channels (e.g., Leverington, 2011). These and other issues can be resolved for Ravi Vallis and other Martian outflow channels by replacing aqueous processes with more realistic mechanisms involving voluminous eruptions of low-viscosity lavas. Volcanic origins are consistent with the basic geological and morphological attributes of the Martian outflow channels (e.g., Schonfeld, 1979; Leverington, 2007, 2009, 2018; Hopper and Leverington, 2014; Leone, 2014, 2017; Baumgartner et al., 2015, 2017), and with the congruence between these attributes and those of ancient volcanic channel systems on other rocky bodies of the inner solar system (e.g., Leveringon and Maxwell, 2004, 2011; 2014; Byrne et al., 2013).

The purpose of this paper is to introduce a volcanic interpretation of the Ravi Vallis channel system, and to highlight the general consistency of the properties of this system with formation by voluminous effusions of low-viscosity lavas. The basic capacity of deep magmatic plumbing systems for development of the Martian outflow channels is outlined, and constraints are placed on the flow conditions, discharge rates, and total lava volumes that might have been involved in the development of Ravi Vallis.

2. Overview of the Ravi Vallis outflow system

Ravi Vallis consists of anastomosing channels that collectively form a relatively small outflow system that varies in width from ~20 to 70 km and extends a total of ~215 km northeastward across Late Noachian cratered plains from Aromatum Chaos (Moore et al., 1995; Wilson et al., 2004; Coleman, 2005; Leask et al., 2006b; Marra et al., 2014; Berman et al., 2018) (Figs. 1–6). Highland plains adjacent to Ravi Vallis are smooth to mottled in appearance, and are associated in places with features such as wrinkle ridges and localized areas of collapse (Berman et al., 2018). Crater counts suggest that Ravi Vallis formed in the Early Hesperian (Berman et al., 2018), or possibly in the Middle-to Late Hesperian (Scott and Tanaka, 1986; Tanaka, 1997; Coleman, 2005; Coleman and Baker, 2009). The absolute age of Ravi Vallis has recently been estimated to be ~3.4 Ga (Berman et al., 2018). The timing of formation of Ravi Vallis relative to that of nearby Shalbatana Vallis remains uncertain

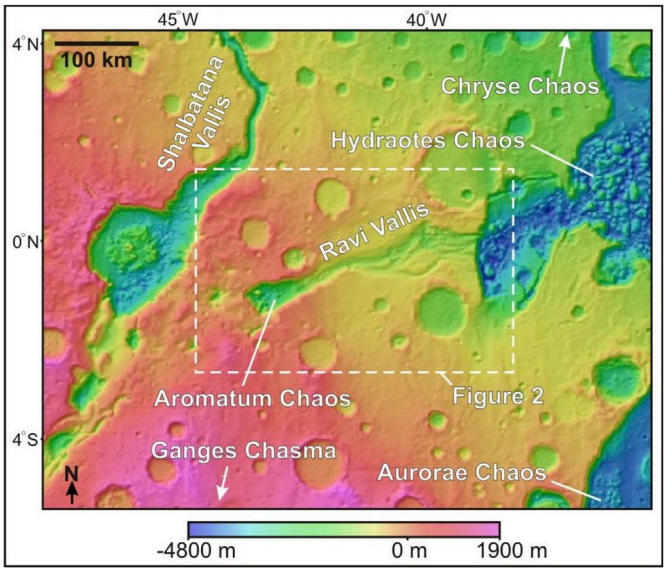

Fig. 1. Mars Orbiter Laser Altimeter (MOLA) topographic map of the Ravi Vallis region (after Smith et al., 2003). The Ravi Vallis system heads at Aromatum Chaos and extends ~215 km northeastward, terminating at Hydraotes Chaos.

(Coleman, 2005). The most distal reaches of Ravi Vallis are truncated by Hydraotes Chaos (Moore et al., 1995; Ori and Mosangini, 1998; Coleman, 2005; Leask et al., 2006a; Coleman and Baker, 2009; Sato et al., 2010), and any channel segments that originally existed beyond this area were destroyed by the later development of Hydraotes Chaos and possibly other features such as Chryse Chaos (Nelson and Greeley, 1999; Coleman, 2005). The original length of Ravi Vallis is unknown.

The topographic depression that contains Aromatum Chaos is ~90 km long and averages ~30 km in width, and is characterized by an interior morphology that is dominated by irregularly-shaped terrain blocks (Fig. 5b) that generally decrease in size toward the eastern end (Leask et al., 2006a). Most of this basin is bounded along its outer perimeter by sharp and relatively steep escarpments that are partly mantled by talus (e.g., Max and Clifford, 2001; Berman et al., 2018) (Fig. 5b). As with other regions of chaos on Mars, the morphology of Aromatum Chaos is suggestive of development through terrain degradation and collapse caused by fluid effusions and by the removal of material in the subsurface (e.g., Sharp, 1973; Moore et al., 1995; Max and Clifford, 2001; Coleman, 2005; Leask et al., 2006a; Andrews-Hanna and Phillips, 2007; Leone, 2014). The deepest parts of the floor of Aromatum Chaos are as great as ~3.4 km below adjacent upland plateaus and ~1.5 km below the proximate floor of Ravi Vallis (Carr, 2012). Upland areas near Aromatum Chaos show signs of disturbance in the form of pits and fracture-like features (e.g., Leask et al., 2006a; Leone, 2014; Sewell et al., 2017) (Figs. 5a and 6f). A prominent lava flow extends southeastward across upland plains from the southern margin of Aromatum Chaos (Figs. 3 and 6b), and crater counts suggest emplacement of this flow in the same approximate time frame as the formation of Ravi Vallis itself (Berman and Rodriguez, 2016; Berman et al., 2018). Sinuous channels with typical widths of ~1 km extend across parts of the uplands adjacent to Aromatum Chaos and Ravi Vallis (Figs. 3 and 6a). The total volume of material estimated to have been lost during development of Aromatum Chaos is ~4090 km^3 (Leask et al., 2006a).

The Ravi Vallis system consists of channels that in places anastamose about streamlined erosional residuals (e.g., Coleman, 2005) (Fig. 5c). Overall, the floors of these channels decrease in elevation by ~300–700 m over the full ~215 km distance between the eastern edge of Aromatum Chaos and the western edge of Hydraotes Chaos, and the system correspondingly has an average longitudinal slope of ~0.1–0.2° (Fig. 4). Terraces are present along some channel margins, channel floors are mantled in places by ponded materials that form smooth plains (e.g., Fig. 6e), and sets of longitudinal ridges that have ridge-to-ridge spacings of ~250–600 m are present along some channel reaches (Leask et al., 2006b; Mangold et al., 2016) (Fig. 5d). Ejecta of the 30-km-diameter Dia-Cau impact crater (Fig. 2) extends across part of the outflow system area but is not present on the floor of Aromatum Chaos or Ravi Vallis, implying that this crater is older than the most recent period of channel development (Leask et al., 2006a). As at other Martian outflow channels (e.g., Chapman et al., 2010a, b; Leverington, 2018), the morphology of the floor of Ravi Vallis suggests initial formation of relatively wide and shallow channels by poorly-confined flows, and the associated deposition of higher-elevation smooth plains materials (Berman et al., 2018) (Figure 3 and Figure 6cd), followed by the gradual incision of deeper and narrower channels within which erosional features are more clearly evident (Coleman, 2005; Leask et al., 2006b; Wilson et al., 2009a). Vertical incision of Ravi Vallis is believed to have exceeded 700 m in places and may have locally reached ~900 m (Wilson et al., 2004; Coleman, 2005; Coleman and Baker, 2009). The total volume of material estimated to have been removed in the development of the Ravi Vallis channel system is ~4190 km^3 (Leask et al., 2006b).

Estimates of thermal inertia can be used to help infer the predominant particle sizes at and near the surface of regions of interest, which can involve combinations of endmembers such as dust (~50 J m^{-2} K^{-1} $sec^{-1/2}$), sand (~225 J m^{-2} K^{-1} $sec^{-1/2}$), duricrust (~900 J m^{-2} K^{-1} $sec^{-1/2}$), and rock (~2500 J m^{-2} K^{-1} $sec^{-1/2}$) (Putzig and Mellon, 2007). Estimates of nighttime thermal inertia based on Thermal Emission

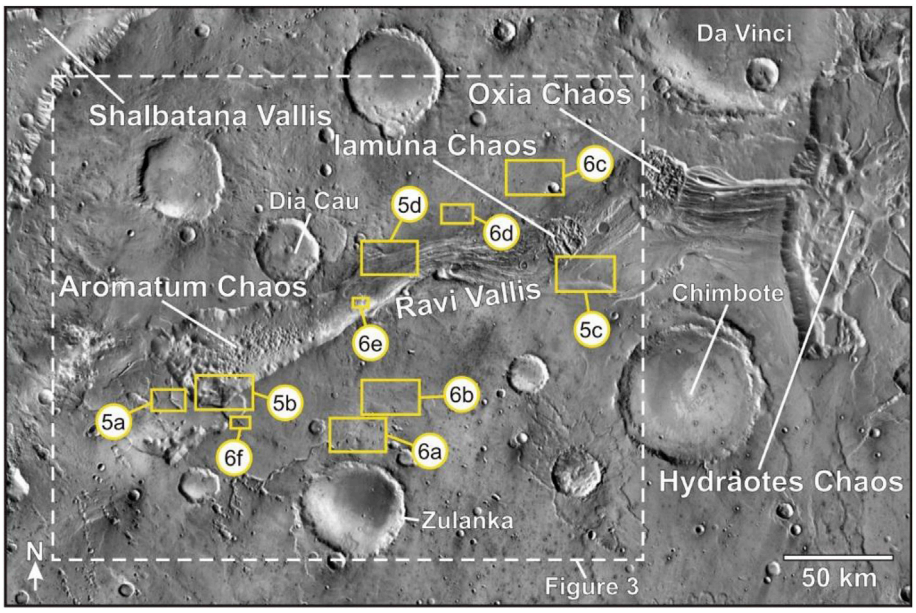

Fig. 2. THEMIS (Thermal Emission Imaging System) daytime infrared mosaic of Ravi Vallis. The depicted area is outlined in Fig. 1. The area depicted in Fig. 3 is indicated, and smaller areas depicted in Figs. 5 and 6 are also given. Mosaic courtesy of Arizona State University.

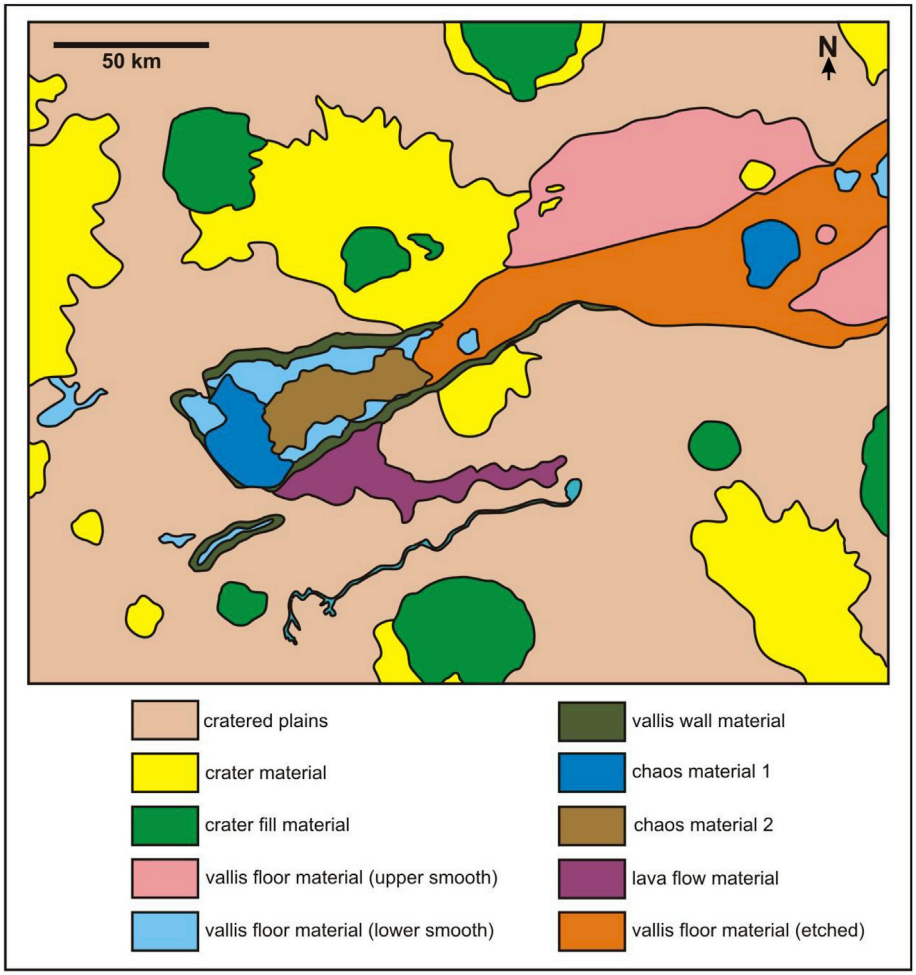

Fig. 3. Geological map of Ravi Vallis (simplified after Berman et al., 2018; see also e.g. Moore et al., 1995). The depicted area is outlined in Fig. 2.

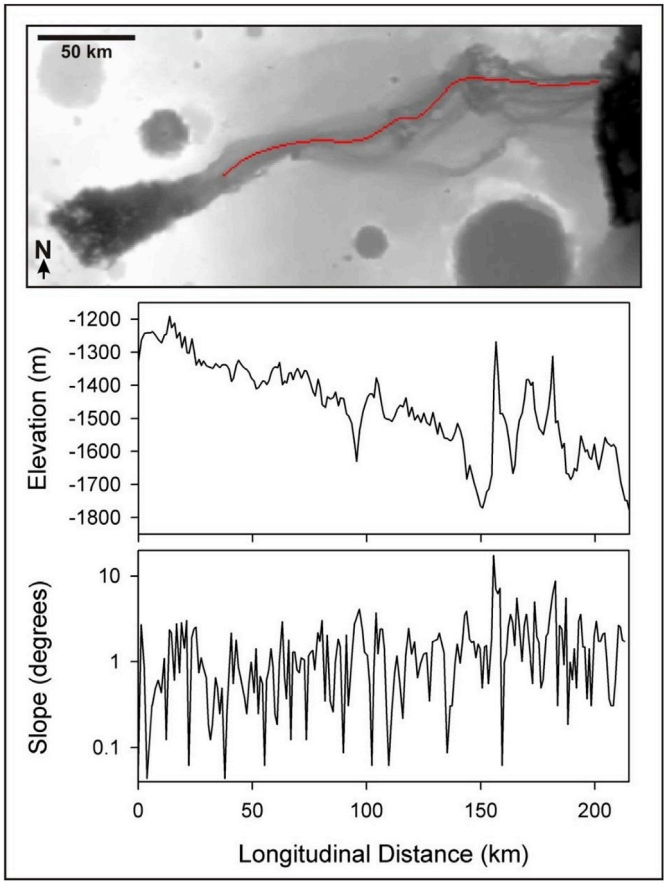

Fig. 4. Elevations and absolute kilometer-scale slopes of Ravi Vallis along one of numerous possible longitudinal paths (red line) (MOLA data after Smith et al., 2003). Slopes along this path are predominantly less than 1°, except where associated with irregular terrain features such as those of Iamuna Chaos and Oxia Chaos (Fig. 2). (For interpretation of the references to colour in this figure legend, the reader is referred to the Web version of this article.)

Spectrometer (TES) and Thermal Emission Imaging System (THEMIS) data mainly range from ~160 to 350 J m^{-2} K^{-1} $sec^{-1/2}$ for the Ravi Vallis system (Putzig and Mellon, 2007; Christensen and Fergason, 2013), suggesting widespread mantling by dust- and sand-sized particles. Immediately beyond the preserved limits of Ravi Vallis, where the channel system sharply transitions to Hydraotes Chaos, exposure of coarser or more consolidated materials is implied by thermal inertia values as great as ~600–850 J m^{-2} K^{-1} $sec^{-1/2}$. Sets of aeolian ripples extend across the interiors of numerous topographic basins in the region (e.g., Fig. 6f). Despite the presence of sedimentary mantles, hydrous silica and smectite clays have been locally identified within the uplands of Xanthe Terra (e.g., Carter et al., 2013; Berman et al., 2018), and olivine-rich volcanic units of Noachian age are in places exposed in the walls and along the floor and adjacent uplands of Ganges Chasma, located south of Ravi Vallis (e.g., Christensen et al., 2003; Edwards et al., 2008).

3. Aqueous interpretations of Ravi Vallis

Aqueous interpretations of Ravi Vallis have mainly involved the hypothesized occurrence of groundwater outbursts produced by the breaching of a confining cryosphere at Aromatum Chaos by tectonic, impact, or igneous events; with resulting channel incision eventually also promoting the release of volatiles, and possibly the development of voluminous secondary outbursts, at Iamuna Chaos and Oxia Chaos (Moore et al., 1995; Nelson and Greeley, 1999; Coleman, 2005, 2016; Leask et al., 2006a, Coleman and Baker, 2009; Wilson et al., 2009a; Rodriguez et al., 2011) (Fig. 2). Outflow of water from the subsurface, perhaps in concert with the melting of local ground ice, is hypothesized to have caused terrain collapse and the related development of chaotic terrain (Coleman, 2005; Leask et al., 2006a). Under aqueous hypotheses, the longitudinal ridges and grooves of Martian outflow channels are generally interpreted as scour features possibly related to longitudinal roller vortices such as those hypothesized to have operated at the Channeled Scablands of Washington (e.g., Baker, 2009). Any absence of expected sedimentary deposits at the Martian outflow channels and within their terminal basins can potentially be attributed to their susceptibility to weathering and erosional processes (e.g., Ghatan and Zimbelman, 2006), to their burial by younger units including lava flows (e.g., Squyres et al., 2004), or to their never having been deposited as prominent landforms as a result of processes such as hyperpychnal flow (e.g., Ivanov and Head, 2001). Formation of both Ravi Vallis and adjacent Shalbatana Vallis has been linked by some workers to the past existence of a deep lake in Ganges Chasma to the south, which is cited as a possible source for replenishment of the aquifer that drove expulsions of water to the surface at Aromatum Chaos (e.g., Carr, 1995, 1996; Cabrol et al., 1997; Nelson and Greeley, 1999; Rodriguez et al., 2003; Coleman, 2003, 2005; Leask et al., 2006a b). Later development of Hydraotes Chaos has been interpreted as a possible consequence of the expulsion of groundwater from an aquifer disrupted by local igneous activity, and the existence here of small cones with summit craters is suggestive of past volcanic activity (Meresse et al., 2007).

Development of both Ravi Vallis and Aromatum Chaos by groundwater outbursts is expected to have involved the removal of ~7200 km^3 of rock and 1100 km^3 of ice, representing a total volumetric loss of ~8300 km^3 (Leask et al., 2006a). Under assumed sediment loads of 10–40% by volume, formation of Aromatum Chaos and Ravi Vallis would have required ~65,000 to 11,000 km^3 of water, respectively (Leask et al., 2006b). Depths of ~50–150 m are postulated for channelized water flows, with estimates of peak water fluxes on the order of ~10^6–10^7 m^3/s (Coleman, 2005; Leask et al., 2006b; Wilson et al., 2009a).

The permeabilities required of some aqueous outburst models range as high as ~10^{-6} to 10^{-7} m^2, which are typical of loose gravel and are up to six or more orders of magnitude greater than might otherwise be expected across large volumes of crust on Mars (Head et al., 2003; Wilson et al., 2009a; Marra et al., 2014). Other models suggest that much lower permeabilities of ~10^{-11} to 10^{-15} m^2 are in fact sufficient for formation of Martian outflow channels and associated regions of chaos (e.g., Andrews-Hanna and Phillips, 2007; Andrews-Hanna et al., 2010). The results of recent work suggests that outbursts of groundwater involving rates sufficiently high to form outflow channels cannot be generated by direct effusions from aquifers without the operation of special processes involving catastrophic releases from groundwater pooled within subsurface voids produced by crustal flexure (Marra et al., 2014). The rupture of this type of flexure-produced subsurface reservoir, with a total volume of 8500 km^3, is proposed by some workers to have driven formation of Ravi Vallis (Marra et al., 2014) and to have involved peak discharges similar to those previously estimated by Leask et al. (2006b).

4. Volcanic formation of the Martian outflow channels

Aqueous models of Martian outflow channel development suffer from numerous shortcomings. For example, there are no known solar system analogs for formation of large channel systems by catastrophic outbursts of groundwater (Leverington, 2011). The largest known aqueous floods on Earth, including those associated with glacial lakes Missoula and Agassiz, were not driven by sudden effusions of water from the subsurface and instead involved releases of water bodies that had been confined by ice dams or other barriers to surface flow (e.g., Bretz, 1969; Leverington et al., 2000, 2002). Despite assumptions of remarkably high sediment loads of ~20–50% (e.g., Komar, 1980; Carr, 1996; Leask et al., 2006b, 2007; Carr and Head, 2015), clear sedimentary evidence for aqueous floods is apparently absent at the outflow channels. Specifically,

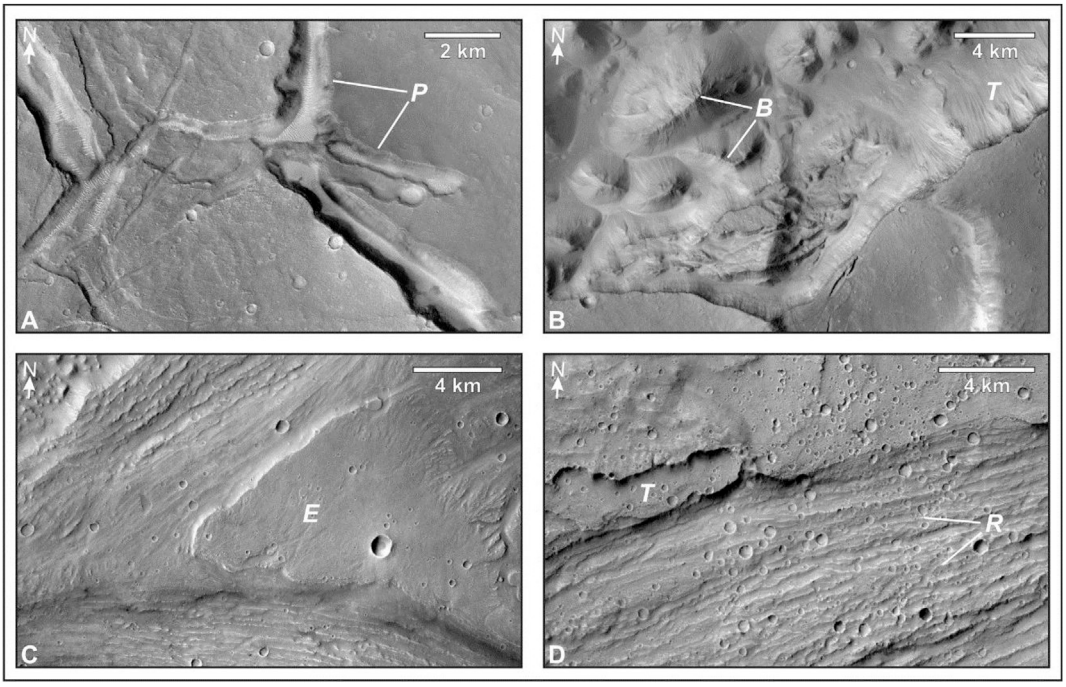

Fig. 5. Examples of landforms associated with Aromatum Chaos (A and B) and Ravi Vallis (C and D): A) fractures and elongate pits on Xanthe Terra uplands located immediately west of Aromatum Chaos; B) terrain blocks and mounds (*B*) and talus materials (*T*) within Aromatum Chaos; C) up-channel extent of an erosional residual (*E*) within Ravi Vallis; D) terrace (*T*) and longitudinal ridges (*R*) within Ravi Vallis. Context Camera (CTX) images: A: D08_030491_1786_XI_01S043W. B: P03_002286_1788_XI_01S043W. C: G03_019533_1809_XN_00N040W. D: P15_006967_1795_XN_00S041W. The locations of depicted areas are given in Fig. 2.

though candidate fluvial deposits continue to be proposed and considered (e.g., Durrant et al., 2017; Hamilton et al., 2018; Kukkonen and Kostama, 2018), obvious examples of fluvial or diluvial sedimentary deposits do not appear to exist along these channel systems (Greeley et al., 1977; Burr and Parker, 2006; Ghatan and Zimbelman, 2006; Leverington, 2007, 2009; 2018; Carling et al., 2009; Hobbs et al., 2011; Leone, 2014, 2017; Rice and Baker, 2015). The outflow channels of Mars lack deltas at their terminal reaches (e.g., Schonfeld, 1977a; Leverington, 2004, 2007; 2011; Leone, 2014, 2017; Rice and Baker, 2015), and though candidate shoreline positions have been proposed for terminal basins (e.g., Parker et al., 1993; Head et al., 1999; Clifford and Parker, 2001; Carr and Head, 2003; Fairén et al., 2003; Di Achille and Hynek, 2010; Rodriguez et al., 2016; Citron et al., 2018), obvious examples of associated depositional features such as beaches, spits, and offshore bars remain elusive (e.g., Malin and Edgett, 1999; Ghatan and Zimbelman, 2006; Leverington, 2011; Pretlow, 2013; Leone, 2014).

Mineralogical evidence in support of aqueous development of the Martian outflow channels is similarly lacking. Global mineralogical evidence confirms the predominance of extremely dry conditions during the interval of outflow channel formation, mainly extending across the Hesperian and well into the Amazonian (e.g., Hoefen et al., 2003; Goetz et al., 2005; Rogers et al., 2005; Bibring et al., 2005, 2006; Koeppen and Hamilton, 2008; Carr and Head, 2010; Hand, 2012; Ehlmann, 2014; Salvatore et al., 2014; Amador et al., 2018). There is extensive preservation of ancient and apparently pristine olivine-rich units in the walls of outflow systems such as Ares Vallis and of deep canyon systems including Valles Marineris (e.g., Christensen et al., 2003; Edwards et al., 2008), despite reliance of aqueous outburst hypotheses on the long-term saturation of the upper ~10 km of the Martian crust and regolith by water variously in its liquid and solid forms (e.g., Baker et al., 1991; Clifford, 1993; Baker, 2001; Clifford and Parker, 2001; Wilson et al., 2009a). There is little correlation between the geographic distribution of Martian outflow channel systems and that of hydrated minerals (e.g., Bibring et al., 2006; Mangold et al., 2008; Carter et al., 2013; Wilson and Mustard, 2013; Ehlmann, 2014), which is very difficult to reconcile with purported aqueous origins for these channels (e.g., Leverington, 2009, 2011; Leone, 2014, 2018), and terminal basins of outflow systems clearly lack the extensive zones of aqueous alteration and evaporite deposition expected of ancient oceans (e.g., Fairén et al., 2011; Mouginot et al., 2012; Pan et al., 2017). Past hydrous environments on Mars (e.g., possible sites of hydrothermal alteration) were markedly restricted in their geographic and temporal extents during the time frame of development of the Martian outflow channels (e.g., Bibring et al., 2006; Christensen et al., 2008; Leverington, 2009, 2011; Leone, 2014, 2018; Cull-Hearth and Clark, 2017; Amador et al., 2018). Even at isolated Martian sites where hydrous minerals are known to be relatively abundant (e.g., sites visited by the Opportunity and Curiosity rovers), the local presence of minerals formed by incomplete processes of diagenesis implies that dry conditions must have prevailed over the billions of years since the time of alteration (e.g., Fairén et al., 2009; Tosca and Knoll, 2009; McLennan, 2012; Rapin et al., 2018). Estimates of Martian near-surface volatile contents from independent mineralogical and geochemical considerations are not congruent with the much larger volumes considered essential for aqueous development of the Martian outflow channels (e.g., Carr, 1986; Carr and Wänke, 1992; Wänke and Dreibus, 1994; Beaty et al., 2005; Carr and Head, 2015; Breuer et al., 2016).

Martian outflow systems head either at ridged volcanic plains or, more typically, at topographic depressions that mark the sites of voluminous fluid effusions from the subsurface, and channel heads are in many cases closely associated with obvious volcanic features and flows (e.g., Plescia, 1990; Keszthelyi et al., 2000, 2004; 2006; Leverington, 2007, 2009; 2011, 2018; Jaeger et al., 2010; Chapman et al., 2010a; Hopper and Leverington, 2014; Leone, 2014, 2017; Hamilton et al., 2018; Korteniemi and Kukkonen, 2018). Component channels extend downslope from source features and are typically partly mantled by volcanic flows, and in most cases terminate in basins that are clearly mantled by thick and extensive flood lavas (e.g., Greeley et al., 1977; Baker, 1982; Carr, 1996; Leverington, 2007, 2011, 2018). The above attributes correspond closely to those of ancient volcanic channels on the

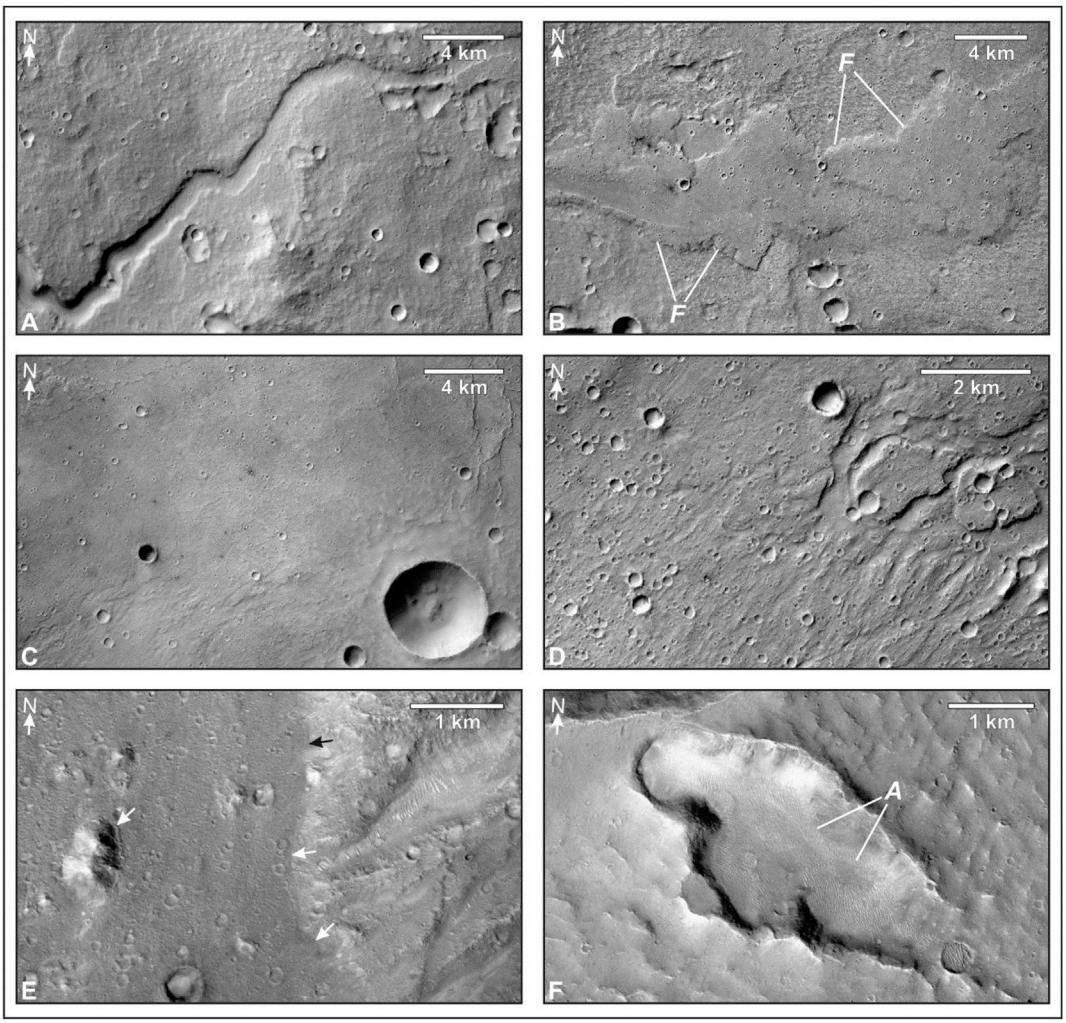

Fig. 6. Examples of likely volcanic landforms within the Xanthe Terra uplands adjacent to Ravi Vallis (A, B, F) and within the Ravi Vallis channel system (C, D, E). A) sinuous channel on Xanthe Terra upland; B) lava flow erupted from the southern margin of Aromatum Chaos (selected flow margins indicated by *F*); C and D) smooth plains materials associated with the northern part of Ravi Vallis; E) Ravi Vallis basin partly filled with dark lobate-margined unit (margins indicated by arrows); F) elongate upland pit with raised margins and interior mantled by extensive aeolian deposits (e.g., light-shaded materials at *A*). CTX images: A: G22_026891_1768_XN_03S042W. B: F20_043572_1786_XN_01S041W. C: J01_045049_1802_XN_00N040W. D: G21_026258_1796_XI_00S041W. E: B11_014008_1795_XN_00S042W. F: D09_030702_1789_XI_01S043W. The locations of depicted areas are given in Fig. 2.

Moon, Venus, Mercury, and Earth (e.g., Leverington, 2004, 2011; 2014; Byrne et al., 2013). Where well preserved and exposed, such volcanic analog systems head at volcanic sources marked by topographic depressions, show evidence for having conveyed lavas along component channels, and terminate at basins mantled by extensive volcanic flows.

Lunar channel systems with lengths of up to hundreds of kilometers and widths of up to ~5 km (e.g., Gornitz, 1973; Wilhelms, 1987; Garry and Bleacher, 2011; Hurwitz et al., 2013a; Roberts and Gregg, 2018) were formed by mafic or ultramafic lavas flowing with minimum viscosities of ~0.5 Pa s and at maximum flow rates of >4000 m^3/s (Murase and McBirney, 1970, 1973; Greeley, 1971; Weill et al., 1971; Hulme, 1973; Hulme and Fielder, 1977; Williams et al., 2000; Hurwitz et al., 2012) (Fig. 7). Venusian systems with lengths of up to thousands of kilometers and widths of up to tens of kilometers (Baker et al., 1992, 1997; Head et al., 1992; Komatsu et al., 1993; Komatsu and Baker, 1994; Komatsu, 2007) were formed by lavas with minimum viscosities at least as low as ~4.5–7.5 Pa s and flow rates as great as ~5×10^7 m^3/s (Kargel et al., 1993; Baker et al., 1997) (Fig. 8). Mercurian systems with lengths of up to ~161 km and maximum widths in excess of 30 km (Head et al., 2011; Byrne et al., 2013) were formed by mafic lavas with viscosities of ~0.02–14.2 Pa s and flow rates as great as ~10^6–10^8 m^3/s (Stockstill-Cahill et al., 2012; Byrne et al., 2013; Hurwitz et al., 2013b) (Fig. 9). Volcanic channels with sizes and properties similar to those of lunar rilles were formed on the Earth during the Archean and Proterozoic by ultramafic lavas with minimum viscosities at least as low as ~0.1–1 Pa s and associated maximum flow rates in excess of ~10^5–10^6 m^3/s (e.g., Williams et al., 2001, 2011). Much larger systems are likely to have developed in the first ~1 Ga of Earth's history (Leverington, 2014).

5. A volcanic interpretation of Ravi Vallis

Clear evidence for development of the Ravi Vallis channel system by groundwater outbursts is lacking. For example, as is the case at other Martian outflow channels (e.g., Rice and Baker, 2015), obvious examples of fluvial or diluvial sedimentary features are not recognized along component channels of this system. Furthermore, the extensive hydrous alteration that would be expected of the aqueous development of Ravi Vallis and other outflow systems (involving an upper crust saturated with groundwater over geological timescales) are apparently missing at exposed olivine-rich uplands and interior walls of Valles Marineris to the south (e.g., Christensen et al., 2003; Edwards et al., 2008; Leverington, 2009; Leone, 2014, 2018; Cull-Hearth and Clark, 2017; Amador et al., 2018). The extensive hydrous alteration and thick mantling by evaporite minerals expected of past sites of large Martian water bodies have not

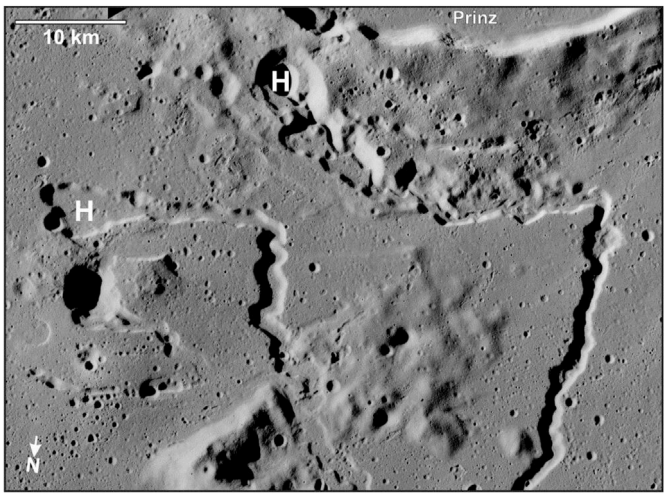

Fig. 7. Two examples of the lunar Rimae Prinz group of sinuous volcanic channels. These systems head at topographic depressions (*H*) that mark the sites of voluminous effusions of low-viscosity lavas (e.g., Hurwitz et al., 2012). Apollo 15 metric camera image 2081.

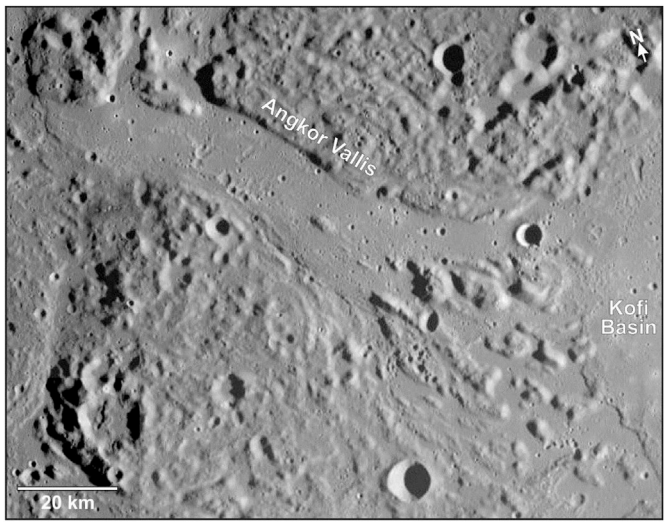

Fig. 9. Angkor Vallis is one of ~10 large volcanic channel systems that developed during emplacement of flood lavas in the northern hemisphere of Mercury (Head et al., 2011; Byrne et al., 2013). Mosaic of MESSENGER (MErcury Surface, Space ENvironment, GEochemistry, and Ranging) Wide Angle Camera images EW0261568757G, EW0246417788G, and EW0231221923G.

been identified within the Chryse basin (e.g., Pan et al., 2017), a basin that is thickly mantled by mare-style flood basalts (e.g., Greeley et al., 1977) and which is likely to have been the ultimate terminal basin of the Ravi Vallis system or the channel systems into which it might have flowed.

Permeabilities expected of the Martian near surface are unlikely to have been sufficient for the development of Ravi Vallis by direct catastrophic effusions from megaregolith aquifers (Marra et al., 2014). Severe disruption of rock units during aqueous outburst events has previously been suggested as a possible means by which permeabilities near the heads of Martian outflow channels could have been increased (e.g., Carr, 1996), but such a mechanism cannot account for the high permeabilities required of aquifers that necessarily extend far beyond the limits of disrupted units (Andrews-Hanna and Phillips, 2007). The hypothesized driving of flood events by releases of groundwater collected in voids produced by crustal flexure can theoretically provide sufficient outflow rates for development of large outflow systems (Marra et al., 2014), but meaningful analogs for catastrophic formation of large aqueous channels by such processes are not known. The development of large crustal voids within which voluminous fluids can collect or be transmitted is a mechanism normally associated with igneous processes, which are a natural outcome of the enormous fluid pressures associated with deeply-rooted magmatic plumbing systems (e.g., Leverington, 2011).

The basic character of the Ravi Vallis channel system is consistent with volcanic origins. The highlands with which this system is associated are characterized by the presence of volcanic landforms such as lava flows and wrinkle ridges (e.g., Berman et al., 2018). The region immediately adjacent to Aromatum Chaos and Ravi Vallis contains localized areas of topographic disturbance including features interpreted as possible maars (Sewell et al., 2017) (though dry volcanic origins for these pits would be more consistent with regional mineralogy), and is also associated with other possible volcanic features such as small sinuous channels. Aromatum Chaos represents a zone of disturbance that marks the site of voluminous fluid effusions from the subsurface. This feature is geographically associated with the canyons of Valles Marineris, which form the most prominent of a radial network of structures centered on the Tharsis volcanic province (Wilson and Head, 2002), and which are interpreted by some workers to have developed through igneous mechanisms that drove volcanic development of several of the largest outflow channel systems of the circum-Chryse region (e.g., Schonfeld, 1979; Leverington, 2011; Leone, 2014). A prominent lava flow extends from the southern margin of Aromatum Chaos and, based on crater counts, was likely erupted from this feature in approximately the same time

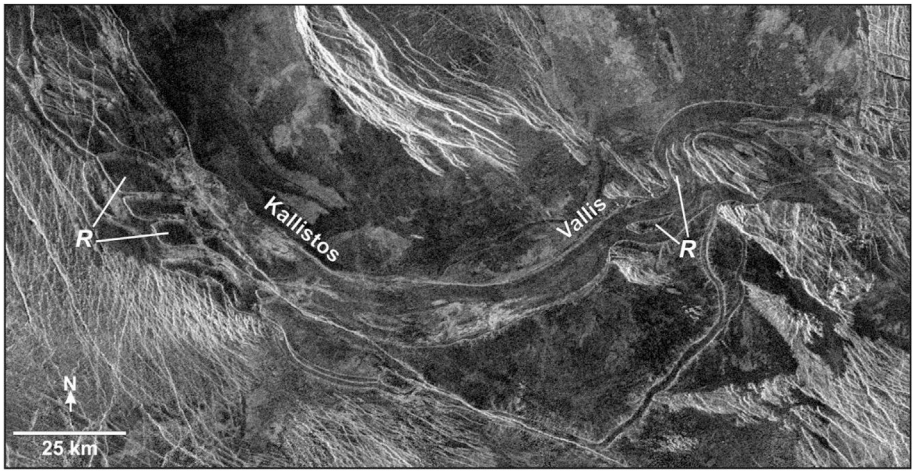

Fig. 8. Middle reaches of Kallistos Vallis, a ~1200-km-long volcanic outflow system located in the Lada Terra region of Venus. This system heads at an extensive zone of chaotic terrain (e.g., Leverington, 2011), and channel segments located downslope of this source are characterized in places by the presence of streamlined erosional residuals (e.g., at *R*) (Baker et al., 1992, 1997; Hopper and Leverington, 2014). Magellan full-resolution radar map (FMAP) left-look synthetic aperture radar mosaic; radar illumination is from the left.

frame as the development of Ravi Vallis (Berman and Rodriguez, 2016; Berman et al., 2018). In places, the various smooth plains units associated with the margins and floors of Ravi Vallis (e.g., Berman et al., 2017, 2018) are characterized by the presence of rille-like channels (e.g., Fig. 6d) and units with lobate flow margins, features which are not uniquely indicative of volcanic origins but are consistent with such an interpretation. The longitudinal ridges and gullies present along the floors of some segments of Ravi Vallis are similar to those present at Athabasca Valles, a Martian channel system interpreted by some workers as having possibly (e.g., Keszthelyi et al., 2017) or certainly (e.g., Leverington, 2011) been developed exclusively by volcanic processes. Under the volcanic interpretation of the Ravi Vallis system, the two additional sites of terrain disturbance located along the Ravi Vallis channel, Iamuna Chaos and Oxia Chaos, are considered likely secondary sites of igneous activity that might have also contributed to channel development.

Analogs for formation of large channel systems by catastrophic releases of groundwater are not known, but the basic properties and geological context of Ravi Vallis are fully aligned with those of ancient volcanic channels of the inner solar system. Disturbance at the heads of volcanic channel systems should result in part from the melting and collapse of country rock during the shallow intrusion of magmas, and channel incision is an expected outcome of voluminous effusions of low-viscosity lavas. For example, lunar and Mercurian channel systems are also associated with igneous source depressions and with channels characterized by features such as terraces and streamlined erosional residuals (e.g., Leverington, 2004, 2011; Head et al., 2011; Byrne et al., 2013). Systems of shallow igneous intrusions can fracture and undermine volcanic units pooled within impact basins on bodies such as the Moon (e.g., Jozwiak et al., 2012; Wilson and Head, 2018), disrupting these units in a manner that does not require the melting of ice and that can superficially resemble that which is characteristic of chaotic terrain on Mars. As with Ravi Vallis, the 1200-km-long Venusian volcanic channel Kallistos Vallis heads at an extensive zone of chaotic terrain and is characterized along numerous reaches by the presence of anastomosing channels and complex sets of streamlined erosional residuals that collectively define extensive scablands (e.g., Baker et al., 1992, 1997; Hopper and Leverington, 2014). Close correspondence with the basic properties expected of large volcanic channels, and the clear capacity of ancient igneous plumbing systems to have driven development of large channels on multiple rocky bodies of the inner solar system through eruption of low-viscosity lavas (e.g., Hulme, 1973, 1974; 1982; Hulme and Fielder, 1977; Huppert et al., 1984; Huppert and Sparks, 1985; Baker et al., 1997; Williams et al., 2000, 2001; 2005, 2011; Jaeger et al., 2010; Hurwitz et al., 2012; Byrne et al., 2013; Dundas and Keszthelyi, 2014; Leverington, 2011, 2014; Hopper and Leverington, 2014; Baumgartner et al., 2015, 2017; Staude et al., 2016, 2017; Lesher, 2017), are consistent with formation of Ravi Vallis by effusions of lava at Aromatum Chaos.

6. Constraints on igneous plumbing systems and surface flow conditions

If the Ravi Vallis channel system formed as a result of voluminous effusions of low-viscosity lavas at Aromatum Chaos, what kinds of igneous processes and flow conditions might have been involved, and what volumes of magma might have been effused to the surface?

6.1. Deeply rooted igneous plumbing systems

Though substantial collapse has taken place at Aromatum Chaos, a relatively deep primary magma source is suggested here by the lack of association with a well-defined set of calderas or a large volcanic cone. Some plume-like environments on Mars, involving the buoyant rise of mantle rock and its partial melting during depressurization, are very likely to have had the capacity to drive production and eruption of magmas at sufficient volumes and rates to form outflow systems (e.g., Leverington, 2007, 2011). On Earth, Large Igneous Provinces are underlain by enormous mafic and ultramafic intrusive bodies that were produced by sublithospheric melting within mantle plumes, and these bodies acted as the sources for later voluminous emplacement of lavas at the surface (e.g., Karlstrom and Richards, 2011). In the absence of excess pressures such as those produced by high rates of magma influx from the mantle below (e.g., Maaløe, 2002), the relatively dense ultramafic melts generated in these terrestrial plume environments are expected to have pooled beneath the crust until magma buoyancy developed as a result of fractional crystallization and the concentration of incompatible volatile species in remaining magmas, eventually leading to the rupture of confining rock units and the progressive development of mafic intrusions that reached the surface and fed large eruptions (Karlstrom and Richards, 2011).

The pooling of melts at deeper rheological boundaries within the uppermost mantle itself (e.g., near the base of the lithosphere) offers an especially attractive mechanism for driving large volumes of mafic or ultramafic magma to the surface in a manner that could have led to development of the Martian outflow channels (Leverington, 2011) (Fig. 10). The development of large intrusion systems from melt zones within the upper mantle is analogously believed to have led to the emplacement of very long mare flows on the Moon and the development of lunar volcanic channels (e.g., Wilson and Head, 2017a, b), as well as the formation of both large and small volcanic features on Mars (e.g., Wilson and Head, 2002; Wilson et al., 2009b; Keszthelyi et al., 2014a; Brustel et al., 2017; Bouley et al., 2018). The positive buoyancy of magma pooled at a rheological boundary within the upper mantle will generate excess pressure at the lower inlet of an associated intrusion system that extends to the surface, and this excess pressure will in many circumstances be sufficiently great to support a column of magma from these depths to the surface (Head and Wilson, 1992; Wilson and Head, 2002, 2017a). The capacity to drive magmas to the surface can be further increased by the existence of mantle melt zones that extend across substantial vertical extents beneath the rheological boundary (Wilson and Head, 2017a) (Fig. 10).

The height to which magma is expected to rise in a connected path from the top of a melt zone located within the upper mantle is given by (Wilson and Head, 2017a):

$$H = [C\ (\rho_{mantle} - \rho_{crust}) - (Z + E)\ (\rho_{mantle} - \rho_{magma})] / \rho_{magma} \quad (1)$$

where H is the depth of the top of an intrusion system (relative to the surface), C is the thickness of the crust, ρ_{mantle} is the density of the upper mantle, ρ_{crust} is the density of the crust, Z is the depth to the top of a melt zone in a shallow mantle, E is the vertical extent of the melt zone, and

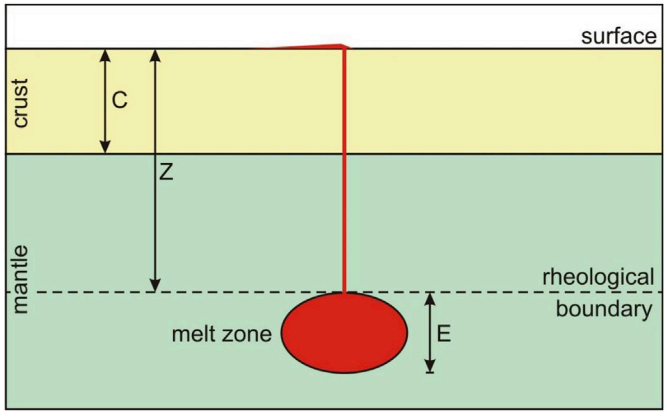

Fig. 10. Schematic illustration of an intrusion system that extends from the top of a melt zone, located at a rheological boundary within the upper mantle, to the Martian surface (modified after Wilson and Head, 2017a). Intrusion systems with these or similar properties are likely to have had the capacity to drive formation of Ravi Valles and other Martian outflow systems. Parameters used in Equations (1) and (2) are defined.

ρ_{magma} is the density of the magma (Fig. 10). H values calculated using Equation (1) are positive if an intrusion system is predicted to stall beneath the surface, and are negative if excess pressures are sufficient to extend an intrusion system above the surface. The magma-driving pressure gradient within an intrusion system is given by (Wilson and Head, 2017a):

$$dP/dz = (g/Z)\,[(Z + E)\,(\rho_{mantle} - \rho_{magma}) - C\,(\rho_{mantle} - \rho_{crust})] \quad (2)$$

where dP/dz is the pressure gradient, and g is gravitational acceleration.

The implications of Equations (1) and (2) for the capacity of deeply-rooted magma systems to deliver magmas to the surface can be illustrated through consideration of several candidate scenarios. The mean crustal thickness of the southern highlands today is estimated to be ~58 km (Neumann et al., 2004), and the mean densities of the Martian crust and upper mantle can be respectively taken to be ~2900 kg/m^3 (McGovern et al., 2002) and ~3500 kg/m^3 (Neumann et al., 2004). Conservatively assuming a magma density of 3000 kg/m^3 (a lower and more buoyant density approaching ~2500 kg/m^3 may be more appropriate for cases involving relatively high volatile contents in magmas; e.g., Brustel et al., 2017) and the existence of a volume of magma sufficient to form a large intrusion system, and assuming that a mantle melt zone is very thin (treated as zero thickness), the mantle melts at the base of a 58-km-thick crust would be expected by Equation (1) to have a capacity to reach no higher than ~1.9 km beneath the Martian surface (in the absence of excess pressures such as those related to high rates of melt influx or changes in buoyancy because of reductions in magma density from fractional crystallization or because of exsolution of volatiles), producing an intrusion that is shallowly stalled within the crust. In contrast, if the very thin melt zone is instead situated at a rheological boundary located more than 11.6 km beneath the base of the crust (i.e., at an overall depth below the surface that exceeds 58 + 11.6 = 69.6 km), magmas would be expected to have sufficient buoyancy to reach the surface as long as sufficient fluid volumes could be drawn from the source region. Thin Martian melt zones at mantle depths greater than 11.6 km would produce progressively greater excess pressures and would more readily be driven to the surface against gravity and wall friction, facilitating the occurrence of voluminous eruptions (for example, the pressure at the inlet of an intrusion system that extends 100 km beneath a 58-km-thick crust would be ~1.93 GPa, and the pressure related to the weight of magma in the intrusion system would be ~1.76 GPa, giving a pressure difference of ~170 MPa and a relatively large associated pressure gradient of 1041 Pa/m).

Still greater excess pressures can be generated by a mantle melt zone with substantial vertical thickness (Wilson and Head, 2017a). The influence of both mantle thickness and melt-zone thickness on the magma-driving pressure gradients of such intrusions is depicted for a 58-km-thick crust in Fig. 11, for mantle thicknesses of 0–100 km and melt-zone thicknesses of 0–40 km. Pressure gradients of ~500 to >1000 Pa/m are sufficient to easily drive mafic or ultramafic magmas to the Martian surface (e.g., Wilson et al., 2009b; Brustel et al., 2017), and such gradients are produced for a wide range of realistic mantle and melt-zone thicknesses (Fig. 11). Intrusion systems with the above properties are realistic candidates for those interpreted to have driven formation of Ravi Vallis and other Martian outflow systems. The specific speed of ascent and overall effusion rate of an intrusion system depend strongly on factors including cross-sectional size of intrusions, which in the case of Aromatum Chaos remains unknown, but Martian intrusions involving low magma viscosities are expected to have had a typical capacity for generating magma rise speeds of 10 m/s or more for intrusion widths of only 3 m (Chevrel et al., 2014).

Mantle plumes can instigate development of enormous radial systems of dikes that converge upon positions of maximum uplift (e.g., Ernst and Buchan, 1997, 2003; Ernst et al., 2005). Large radial extensional structures are centered on the Tharsis and Elysium volcanic provinces (e.g., Hall et al., 1986; Wilson and Head, 2002), and the association of outflow

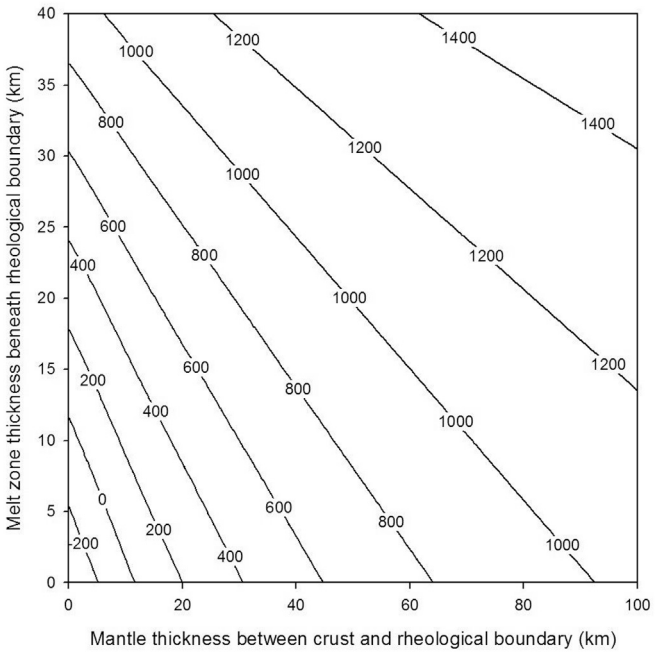

Fig. 11. Estimated magma-driving pressure gradients (dP/dz in Pa/m) for a 58-km-thick Martian crust and for a range of possible underlying mantle thicknesses and melt-zone thicknesses. Mantle thickness refers to the amount of mantle within which the upper part of an intrusion system is rooted (Z minus C in Fig. 10), and melt-zone thickness refers to the thickness of mantle within which melts are generated and that underlies the intrusion system (E in Fig. 10). Plumbing systems associated with thickness parameters of the depicted magnitudes can readily generate pressure gradients of ~500 to >1000 Pa/m, which are certainly sufficient to have driven low-viscosity magmas from large Martian magma chambers to the surface with high rates of flow (e.g., Wilson et al., 2009b; Brustel et al., 2017).

systems with these structures (e.g., Mangala Valles, Athabasca Valles, and Hrad Vallis), suggests possible development of these systems in association with eruptions produced in plume-like environments (e.g., Leverington, 2007, 2011; Hopper and Leverington, 2014). Aromatum Chaos lacks morphological properties suggestive of development in association with a single narrow dike, but the close spatial association of Ravi Vallis with the Valles Marineris fracture system, which itself consists of the most prominent parts of a greater Tharsis-radial system of structures and intrusions, suggests that its development may also have nevertheless been related to a Tharsis plume. The circum-Chryse outflow channel systems are closely associated with Valles Marineris, suggesting a close genetic relationship driven by igneous processes (e.g., Schonfeld, 1979; Leverington, 2011; Leone, 2014).

6.2. Flow volumes and conditions

Flows associated with the Martian outflow channels are of mafic or ultramafic composition (e.g., Greeley et al., 1977; Gellert et al., 2004; Mangold et al., 2010; Jaeger et al., 2010). Partly on the basis of elemental abundances measured in situ for Martian volcanic rocks, at least some of these flows are expected to have been emplaced with minimum viscosities approaching ~0.5 Pa s or less (e.g., Chevrel et al., 2014), which for voluminous flows would certainly have promoted the occurrence of turbulent flow and channel incision (e.g., Schonfeld, 1977a, b; Hurwitz et al., 2010; Jaeger et al., 2010; Leverington, 2014, 2018; Dundas and Keszthelyi, 2014; Hopper and Leverington, 2014; Cataldo et al., 2015; Baumgartner et al., 2015, 2017). Channel incision is expected to have involved both thermal processes (involving the melting of substrates) and mechanical processes (involving the weathering and erosion of substrates by kinetic energy) (e.g., Keszthelyi and Self, 1998; Williams et al., 1998,

2000; Hurwitz et al., 2010; Dundas and Keszthelyi, 2014; Cataldo et al., 2015; Baumgartner et al., 2017). Though exotic by modern terrestrial standards, silicate lavas with minimum viscosities spanning the range of ~0.01–10 Pa s are expected to have been involved in ancient periods of channel incision on all large rocky bodies of the inner solar system including the Earth (e.g., Hulme, 1973; Hulme and Fielder, 1977; Lesher and Campbell, 1993; Baker et al., 1997; Barnes, 2006; Houlé et al., 2008, 2012; Hurwitz et al., 2012; Byrne et al., 2013; Gole et al., 2013; Hurwitz et al., 2013b; Baumgartner et al., 2015, 2017; Staude et al., 2016, 2017; Lesher, 2017) (see Section 4 above).

Lunar igneous plumbing systems rooted at subcrustal depths are estimated to have had the capacity to easily drive basalts to the surface at rates at least as great as ~10^4–10^6 m^3/s (e.g., Wilson and Head, 2017a,b), which would have been sufficient to drive maximum sustained flow rates of >4000 m^3/s at lunar volcanic channels (e.g., Hulme, 1973; Hulme and Fielder, 1977; Williams et al., 2000; Hurwitz et al., 2012). Still greater effusion rates would have been required in order to support maximum estimated channelized discharge rates of ~5×10^7 m^3/s on Venus (e.g., Kargel et al., 1993; Baker et al., 1997) and ~10^6–10^8 m^3/s on Mercury (e.g., Stockstill-Cahill et al., 2012; Byrne et al., 2013; Hurwitz et al., 2013b). Flow crusts should have a capacity to insulate flows and reduce cooling to as little as 1 °C per 30 km for flows with depths of 20–30 m (e.g., Keszthelyi et al., 2006), allowing high-volume lavas to flow for up to thousands of kilometers (e.g., Leverington, 2018). On this basis, voluminous insulated lavas may have cooled as little as ~7 °C along the full 215-km-length of the preserved Ravi Vallis system.

The total volume of material removed during development of Aromatum Chaos is ~4090 km^3 (Leask et al., 2006a), and the total volume of material removed in the development of the Ravi Vallis channel system is ~4190 km^3 (Leask et al., 2006b), giving a total lost volume of ~8280 km^3. On the basis of thermal considerations, recent work has suggested minimum required volumes of erupted lava of ~8–25 times the volume of material removed within a given channel system (Leverington, 2007, 2018; see also Keszthelyi and Self, 1998; Keszthelyi et al., 2014b; Cataldo et al., 2015). This suggests a minimum requirement of ~31,700 to 102,250 km^3 of erupted lava for Aromatum Chaos and ~32,500 to 104,750 km^3 of erupted lava for the Ravi Vallis channel system, for a total minimum erupted volume of ~64,000 to 207,000 km^3. The original length of the Ravi Vallis channel system is unknown, and the volume of erupted lava required for formation of this system would necessarily increase with greater assumed lengths.

Unlike large Martian outflow systems such as Kasei Valles, which is known to have formed over an extended period of geological time (e.g., Chapman et al., 2010a), the Ravi Vallis system is sufficiently modest in size that it may have been formed by a small number of eruptive events over a relatively short period of geological time. What conditions might have characterized channelized flows, and approximately how long might development of the channel system have taken? Key aspects of the manner in which channelized lavas flow and incise into substrates are not yet well understood, and available numerical tools must correspondingly be used with caution (e.g., Dundas and Keszthelyi, 2014; Cataldo et al., 2015). In this work, a set of equations (Hurwitz et al., 2010, 2012; Leverington, 2014, 2018; Hopper and Leverington, 2014) was used in an effort to better constrain the flow conditions and rates of incision that might have been involved in development of the Ravi Vallis system. These equations are functions of each other and must be solved iteratively until variables converge upon particular solutions.

Mechanical incision by a flow (Sklar and Dietrich, 1998; Hurwitz et al., 2010, 2012) is given by:

$$\left(\frac{\mathrm{d}(d_{\mathrm{chan}})}{\mathrm{d}t}\right)_{\mathrm{mechanical}} = K\,\rho\,g\,Q_{\mathrm{w}}\,sin\alpha. \tag{3}$$

where K quantifies the erodibility of a substrate in Pa^{-1}, ρ is the density of lava, g is gravitational acceleration, Q_w is the discharge of lava per meter of channel width (given in m^2/s), and α is the channel slope in degrees. For slopes of <10°, the velocity of a flow (Keszthelyi and Self, 1998; Hurwitz et al., 2010, 2012) is given by:

$$(v_{lava})^2 = \frac{g\,d_{lava}\,sin\alpha}{C_f} \tag{4}$$

where g is gravitational acceleration, d_{lava} is the depth of lava, α is the channel slope, and C_f is the friction factor (Keszthelyi and Self, 1998), which is given by:

$$C_f = \left(\frac{1}{32}\right)\left(log_{10}\left[6.15\left(\left(\frac{2Re+800}{41}\right)^{0.92}\right)\right]\right)^{-2} \tag{5}$$

with the Reynolds number (Re) given by:

$$Re = \frac{\rho\,v\,d_{lava}}{\mu} \tag{6}$$

where ρ is the density of lava, υ is the velocity of lava, d_{lava} is the depth of lava, α is the channel slope, and μ is the dynamic viscosity of lava.

Thermal incision by a flow (Hulme, 1973; Huppert and Sparks, 1985; Williams et al., 1998, 2000; Hurwitz et al., 2012) is given by:

$$\left(\frac{\mathrm{d}(d_{\mathrm{chan}})}{\mathrm{d}t}\right)_{\mathrm{thermal}} = \frac{h_{\mathrm{T}}(T - T_{\mathrm{mg}})}{E_{\mathrm{mg}}}. \tag{7}$$

where h_T is the coefficient of heat transfer, T is the temperature of lava, T_{mg} is the temperature at which the substrate melts, and E_{mg} is the energy required to melt the substrate (Hulme, 1973; Huppert and Sparks, 1985; Williams et al., 1998, 2000):

$$E_{mg} = \rho_{\mathrm{g}}\left[c_{\mathrm{g}}(T_{\mathrm{mg}} - T_{\mathrm{g}}) + f_{\mathrm{mg}}\,L_{\mathrm{g}}\right] \tag{8}$$

where ρ_g is the density of the substrate, c_g is the specific heat of the substrate, T_{mg} is the temperature at which the substrate melts, T_g is the initial temperature of the substrate, f_{mg} is the fraction of the substrate that must be melted prior to mobilization, L_g is the latent heat of fusion of the substrate; and h_T is the coefficient of heat transfer (Hulme, 1973; Hurwitz et al., 2012), which is given by:

$$h_T = \frac{0.017\,k\,Re^{\frac{4}{5}}\,Pr^{\frac{2}{5}}}{d_{lava}} \tag{9}$$

where k is the thermal conductivity of lava [2.16 – (0.0013 T)] (Williams et al., 1998), Re is the Reynolds number, Pr is the Prandtl number [$(c_g\mu)/k$], and d_{lava} is the depth of lava.

Equation parameters used to model flow conditions are given in Table 1. The proportionality constant (K) was assigned a value of 10^{-9}, which corresponds to a strong bedrock substrate (e.g., Hurwitz et al., 2012). Average lava flow depths of ~20 m have been estimated for Athabasca Valles (Jaeger et al., 2010), but local lava depths of up to hundreds of meters are considered realistic for some channel systems (e.g., Jaeger et al., 2010; Byrne et al., 2013; Dundas and Keszthelyi, 2014), and depths of ~50–150 m were previously inferred for channelized water flows at Ravi Vallis (Coleman, 2005; Leask et al., 2006b; Wilson et al., 2009a). In the present study, lava depths of 25 and 50 m were used in flow calculations. Minimum lava viscosities of ~0.01–10 Pa s are expected to have been involved in channel incision in the inner solar system (e.g., Murase and McBirney, 1970, 1973; Kargel et al., 1993; Williams et al., 2000, 2011; Barnes, 2006; Houlé et al., 2008, 2012; Hurwitz et al., 2012; Stockstill-Cahill et al., 2012; Baumgartner et al., 2017), and a viscosity of 1 Pa s is favored here for channel reaches closest to Martian volcanic sources (e.g., Hopper and Leverington, 2014; Leverington, 2014, 2018); viscosities of 1 Pa s, 50 Pa s, and 500 Pa s were used in flow calculations. Lava temperatures approaching or in excess of 1400 °C are very likely for at least some ancient mafic and ultramafic lavas involved in channel development (e.g., Burns and Fisher, 1990;

Table 1
List of constants and variables.

Symbol	Name	Units	Value
K	Proportionality constant of substrate erodibility	Pa^{-1}	10^{-9} (bedrock)
ρ	Density of lava	kg/m^3	2800
g	Gravitational acceleration	m/s^2	3.7
Q_w	Discharge per meter width	m^2/s	calculated
α	Longitudinal slope	degrees	0 to 1
v	Velocity of lava	m/s	calculated
d_{lava}	Depth of lava	m	25 and 50
C_f	Friction factor	none	calculated
Re	Reynolds number	none	calculated
μ	Dynamic viscosity	Pa s	1
h_T	Heat transfer coefficient	$(J\ m^2)/(s\ K)$	calculated
T	Temperature of lava	°C	1350
T_{mg}	Substrate melting temperature	°C	1150
E_{mg}	Energy needed to melt substrate	J/m^3	calculated
ρ_g	Density of solid substrate	kg/m^3	2900
c_g	Specific heat of substrate	J/(kg °C)	1500
T_g	Initial temperature of ground	°C	−23
f_{mg}	Fraction of substrate melting required for mobilization	none	0.4 (40%)
L_g	Latent heat of fusion of substrate	J/kg	587,000
k	Thermal conductivity of lava	W/(m K)	calculated

Nisbet et al., 1993; Grove and Parman, 2004; Filiberto et al., 2008; Williams et al., 2011; Baumgartner et al., 2015, 2017) and a lava temperature of 1350 °C was used in flow calculations here. Kilometer-scale slopes of under 1° are typical of the Ravi Vallis system for reaches that did not become affected by the later development of features such as patches of chaotic terrain (Fig. 4), and slopes of 0.0–1.0° were therefore used in flow calculations.

Flow conditions estimated on the basis of Equations (3)–(9) are given in Fig. 12. Results are given for slopes of up to 1°, but volcanic channels should have a strong tendency to develop especially low slopes along component channels as they mature (e.g., Leverington, 2014) and conditions involving slopes of $< \sim 0.4°$ are therefore expected to have been particularly relevant to the overall development of Ravi Vallis and most other Martian outflow channels (e.g., Leverington, 2018). Though flow velocities are predicted to reach as great as 60 m/s for 50-m-deep flows on slopes of 1°, for more representative slopes of 0.2°, velocities for 25-m-deep and 50-m-deep flows are expected to respectively reach as great as ~17 and 26 m/s. For lavas with viscosities of 1 Pa s, flow conditions are predicted to be fully turbulent for all slopes, with maximum Reynolds numbers of $\sim 8.5 \times 10^6$ estimated for 50-m-deep flows on slopes of 1°; in comparison, lavas with viscosities of 500 Pa s are predicted to have relatively laminar flow characteristics ($Re < 3000$) for slopes of less than 1° (25-m-deep flows) and less than 0.15° (50-m-deep flows). Mechanical and thermal incision rates are respectively predicted for viscosities of 1 Pa s to be as great as ~47 and 3.8 m/day for 50-m-deep flows on slopes of up to 1°. For more representative slopes of 0.2°, mechanical incision rates for 25-m-deep and 50-m-deep flows with viscosities of 1 Pa s are respectively predicted to be associated with incision rates of ~1.3 and 4.0 m/day, and thermal incision rates are respectively predicted to be associated with incision rates of ~1.6 and 1.9 m/day. Consistent with earlier work (e.g., Hurwitz et al., 2012), mechanical incision rates are generally expected to exceed thermal rates for all but the lowest slopes, and thermal incision rates are especially low for relatively high lava viscosities (e.g., for lavas with viscosities of 500 Pa s, thermal incision rates of under 0.2 m/day are predicted on slopes of less than 1°).

Discharge rates are given in Fig. 13 for flows with an assumed width of 25 km, which is the approximate average width of the main Ravi Vallis channel system. For lavas with viscosities of 1 Pa s and flowing on slopes of 1°, discharge rates are predicted to be $\sim 24.7 \times 10^6\ m^3/s$ and $75.7 \times 10^6\ m^3/s$ for flows with depths of 25 m and 50 m, respectively. On more representative slopes of 0.2°, discharge rates are respectively predicted to be $\sim 10.3 \times 10^6\ m^3/s$ and $31.8 \times 10^6\ m^3/s$ for flows with these depths and viscosities. Flows with viscosities of 500 Pa s are predicted to have discharge rates that are roughly half those of flows with viscosities of 1 Pa s.

The manner in which mechanical and thermal incision processes interact is not well understood or easily quantified, complicating estimation of overall incision rates. Net incision rates will also be reduced in some cases by the capacity of lower-volume or higher-viscosity lava flows to constructively emplace volcanic units rather than to incise into substrates (e.g., Leverington, 2007), potentially resulting in the emplacement of solid volcanic mantles that must later be weathered and eroded by subsequently erupted lavas. Conservatively assuming a net combined mechanical and thermal incision rate of only 1.5 m/day (Leverington, 2018) and an average total amount of incision across Ravi Vallis of 700 m (Wilson et al., 2004; Coleman, 2005; Coleman and Baker, 2009), a total lava effusion volume of ~167,000 km^3 is predicted for this system on the basis of the discharge value of ~4,150,000 m^3/s predicted to be associated with flows with viscosities of 1 Pa s, widths of 25 km, depths of 25 m, and slopes of 0.2°. Under these rudimentary assumptions, incision of the preserved 215-km-long segment of the Ravi Vallis system is estimated to have required a total of ~470 days, though channel development could have taken place in a series of separate events of shorter duration that were spaced over geological lengths of time. The total estimated effusion volume of ~167,000 km^3 falls within the minimum range of ~64,000 to 207,000 km^3 estimated separately on the basis of thermal considerations.

7. Discussion

The volumes of lava estimated to have been required for formation of Ravi Vallis are similar in magnitude to those typical of the smallest terrestrial Large Igneous Provinces. For example, though estimated volumes represent well under 1% of the preserved $\sim 5 \times 10^7\ km^3$ of the Ontong Java Plateau (Coffin and Eldholm, 1993), they represent ~30%–100% of the preserved 210,000 km^3 volume of the Columbia River Basalt Group (Camp et al., 2017). The extensive but relatively shallow Martian outflow system Athabasca Valles is mantled by only ~7500 km^3 of lava (Jaeger et al., 2010), and the narrow Hrad Vallis system is estimated to have been formed by effusion of as little as ~10,900 km^3 of lava (Hopper and Leverington, 2014). Greater total effused lava volumes of $\sim 2 \times 10^5\ km^3$ and $5 \times 10^6\ km^3$ are respectively estimated for formation of the Martian outflow systems Mangala Valles (Leverington, 2007) and Kasei Valles (Leverington, 2018).

On slopes of 0.2°, lava flows with assumed viscosities of 1 Pa s, temperatures of 1350 °C, and depths of 50 m, are estimated to have been associated at Ravi Vallis with maximum lava discharge rates of $\sim 3 \times 10^7\ m^3/s$, which are similar in magnitude to the maximum aqueous flow rates previously calculated for this system (Coleman, 2005; Leask et al., 2006b; Wilson et al., 2009a). Such flow rates are greater than the peak rates of up to $\sim 8.7 \times 10^3\ m^3/s$ estimated for the 1783–1784 Laki fissure eruption of Iceland (Thordarson and Self, 1993) and the rates of up to $\sim 10^6\ m^3/s$ estimated for some units of the Columbia River Basalt Group (Reidel, 1998), but are similar to those previously estimated for other large volcanic channel systems of the inner solar system. For example, rates possibly greater than $10^6\ m^3/s$ are estimated for Archean channel-forming flows of the Perseverance ultramafic complex (Western Australia) (Williams et al., 2001) and Proterozoic channel-forming flows of the Cape Smith Belt (Quebec) (Williams et al., 2011), rates of up to $\sim 5 \times 10^7\ m^3/s$ are estimated for formation of Venusian channel Kallistos Vallis (Baker et al., 1997), rates of up to $\sim 1.7 \times 10^8\ m^3/s$ are estimated for formation of Martian outflow system Athabasca Valles (Jaeger et al., 2010), and rates of up to $\sim 1.7 \times 10^8\ m^3/s$ are estimated for formation of the Mercurian channel systems (Byrne et al., 2013). Lava incision rates of up to tens of meters per day for slopes of up to 1° are consistent with previous estimates made for ancient volcanic channels on Earth (e.g., Williams et al., 2001, 2011; Leverington, 2014), the Moon (e.g., Hurwitz

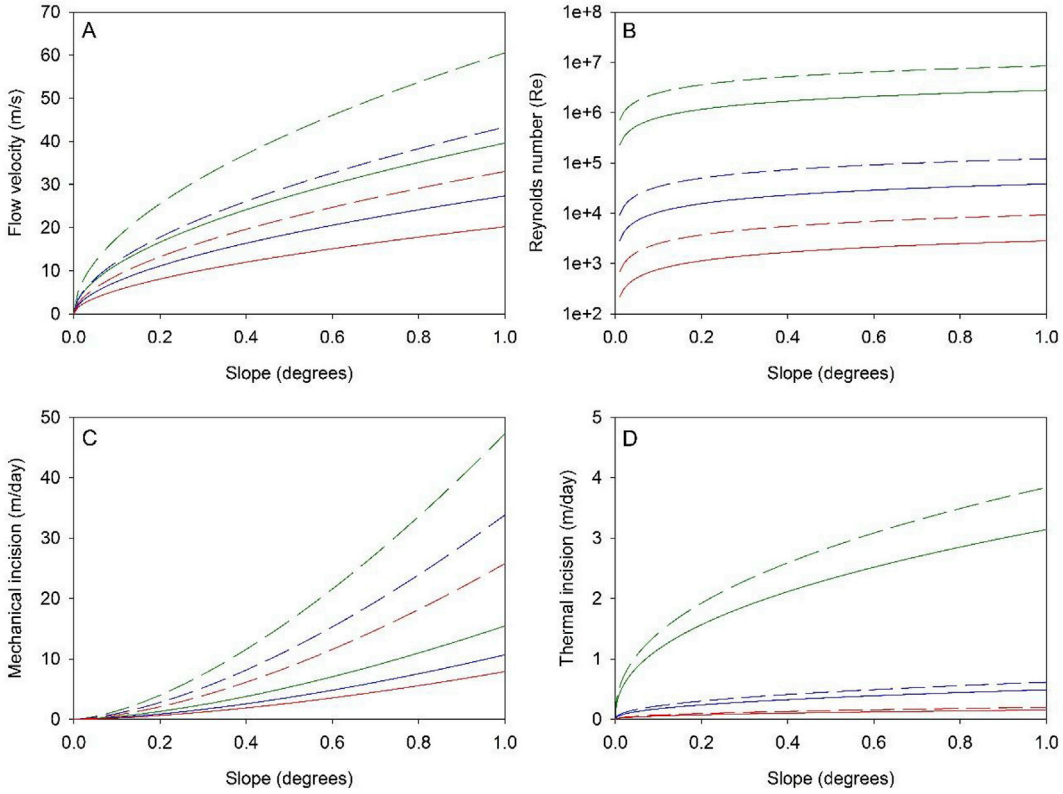

Fig. 12. Predicted flow conditions for 50-m-deep flows (dashed lines) and 25-m-deep flows (solid lines), assuming a strong bedrock substrate and lava viscosities of 1 Pa s (green), 50 Pa s (blue), and 500 Pa s (red); for lava temperatures of 1350 °C. A: flow velocity; B: flow turbulence (semi-log plot); C: mechanical incision rate; D: thermal incision rate. There is a strong tendency of volcanic channels to have kilometer-scale slopes of well under 1° (e.g., Leverington, 2014), and conditions involving slopes of < ~0.4° are expected to have been especially relevant to the overall development of Ravi Vallis and most other Martian outflow systems. For some channel systems, much steeper slopes can be associated with local features such as cataracts, and the capacity for weathering and erosion will be greatly enhanced in such environments (e.g., Dundas and Keszthelyi, 2014; Dundas et al., 2019). (For interpretation of the references to colour in this figure legend, the reader is referred to the Web version of this article.)

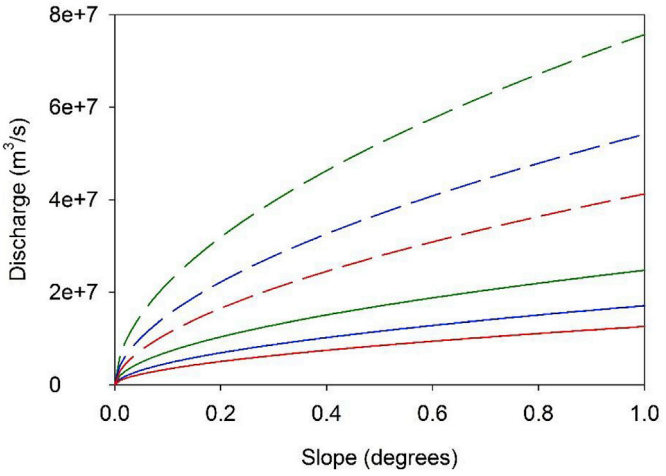

Fig. 13. Estimated discharge rates for 50-m-deep flows (dashed lines) and 25-m-deep flows (solid lines) for lavas with viscosities of 1 Pa s (green), 50 Pa s (blue), and 500 Pa s (red). Flow widths of 25 km are assumed. (For interpretation of the references to colour in this figure legend, the reader is referred to the Web version of this article.)

et al., 2012), Mercury (e.g., Hurwitz et al., 2013b), and Mars (e.g., Hopper and Leverington, 2014; Baumgartner et al., 2017; Leverington, 2018). Lava flows are conservatively estimated to have had a capacity to form Ravi Vallis in ~470 days (possibly involving individual events separated by geological spans of time), which is greater than the ~17 days estimated to have been most efficiently involved in development of Athabasca Valles (Jaeger et al., 2010) and less than the ~1000 days estimated for development of Kasei Valles (again, with individual eruptive events separated by much larger periods of geological time) (Leverington, 2018).

Though Ravi Vallis is a relatively small outflow channel, its mechanisms of formation are relevant to our understanding of the fundamental attributes and geological history of Mars. Specifically, a volcanic origin for Ravi Vallis is consistent with the wider interpretation of all Martian outflow channels as products of voluminous effusions of low-viscosity lavas (Schonfeld, 1977a, b, 1979; Leverington, 2004, 2007, 2009, 2011, 2014, 2018; Hopper and Leverington, 2014; Leone, 2014, 2017, 2018; Baumgartner et al., 2015, 2017). Past development of all Martian outflow channels by dry volcanic processes, rather than by aqueous floods or by hybrid processes involving both volcanic and aqueous flows, is consistent with the general absence at these systems of expected sedimentary deposits, extensive aqueous alteration, and thick evaporite deposits. Volcanic origins for the Martian outflow channels are also aligned with the analogous past development of hundreds of volcanic outflow systems on rocky bodies of the inner solar system (e.g., Leverington, 2004, 2011), and with the premise that early development of immense volcanic channel systems is typical of all large rocky bodies in and beyond our solar system (Leverington, 2014).

The foundering of past aqueous interpretations of the outflow channels suggests that assumptions of aqueous origins should also be reconsidered for other Martian channel types. For example, upland channel systems and valley networks on Mars, like their outflow counterparts, lack special geographic correlations with the presence of hydrous minerals (e.g., Bibring et al., 2006; Ehlmann, 2014), and overall, the Martian

surface has undergone remarkably little alteration by water (e.g., Christensen et al., 2008). Though heavily-cratered Noachian terrains are widely associated with clays, available data suggest the early formation of these minerals in the subsurface under conditions involving low ratios of water to rock, rather than by surface weathering involving precipitation and runoff (Ehlmann et al., 2011). Furthermore, recent climate models based on realistic assumptions fail to predict the warm and wet conditions considered essential for formation of Martian channels and valley networks by precipitation and surface runoff (Wordsworth, 2016). Where exposure is good, channel features such as those routinely interpreted as lacustrine deltas are in many cases lacking in expected spectral signatures of aqueous alteration, associated closed basins are missing expected evidence for evaporite deposition, and convincing evidence for the existence of lacustrine shorelines or terraces is absent (Goudge et al., 2015). Notably, as with the outflow channels, numerous upland channel systems and valley networks on Mars, including many previously hypothesized to have formed in association with crater lakes, show evidence for development as products of extensive volcanic resurfacing involving low-viscosity lavas (e.g., Leverington and Maxwell, 2004; Leverington, 2005, 2006). To what extent were Martian channels of all kinds formed by mainly or entirely dry processes? Even the formation of small Martian gullies appears on the basis of recent work to be a dry process (e.g., Dundas et al., 2017). Dry interpretations of most or all Martian channel systems, if valid, would reduce or eliminate the need to hypothesize enormous subsurface reservoirs of water and the past occurrence of transient periods of planet-wide warm and wet conditions, and would instead be consistent with the predominance of cold and dry surface conditions over the history of Mars.

8. Conclusions

Ravi Vallis is a Martian outflow channel that formed in the Hesperian as a result of fluid outflows from adjacent Aromatum Chaos. Though this system is widely interpreted as a product of catastrophic outbursts from aquifers, hypothesized aqueous processes lack meaningful solar system analogs, and the system lacks obvious sedimentary and mineralogical signatures expected of aqueous origins. Instead, the basic attributes of Ravi Vallis are aligned with those typical of volcanic channels of the inner solar system, and are consistent with volcanic origins involving voluminous effusions of low-viscosity lavas at Aromatum Chaos.

Igneous plumbing systems rooted in the upper Martian mantle are expected to have had a broad capacity to generate pressure gradients necessary for the eruption of large lava volumes at the heads of outflow systems including Ravi Vallis, and eruptions from large magma chambers stranded at depths of ~90 km or more would in particular have had a capacity to generate pressure gradients well in excess of 500 Pa/m. Lava flows with viscosities of 1 Pa s, temperatures of 1350 °C, and depths of 50 m, are predicted to have had the flow characteristics necessary to drive incision into strong bedrock substrates at rates of at least several meters per day on slopes of well under 1°, and maximum associated discharge rates are likely to have been $\sim 3 \times 10^7\ m^3/s$ for flows with widths of ~25 km on slopes of 0.2°. Combined development of Aromatum Chaos and the preserved extent of Ravi Vallis is estimated to have required eruption of a minimum of ~64,000 km^3 of lava. The original length of the preserved 215-km-long channel system is not known, and greater lava volumes would have been required for formation of its full past extent.

A volcanic origin for Ravi Vallis is consistent with development of all Martian outflow channels by volcanic processes involving effusion of low-viscosity lavas, and with the broader premise that development of immense volcanic channel systems is typical of the early histories of all large rocky bodies. A dry origin for the outflow channels of Mars would imply that near-surface water reservoirs on this planet are much less voluminous than previously hypothesized, and would be consistent with the predominance of cold and dry surface conditions over the history of Mars.

Acknowledgements

The helpful comments of two anonymous reviewers are appreciated.

References

Amador, E.S., Bandfield, J.L., Thomas, N.H., 2018. A search for minerals associated with serpentinization across Mars using CRISM spectral data. Icarus 311, 113–134.
Andrews-Hanna, J.C., Phillips, R.J., 2007. Hydrological modeling of outflow channels and chaos regions on Mars. J. Geophys. Res. 112, E08001 https://doi.org/10.1029/2006JE002881.
Andrews-Hanna, J.C., Zuber, M.T., Arvidson, R.E., Wiseman, S.M., 2010. Early Mars hydrology: meridiani playa deposits and the sedimentary record of Arabia Terra. J. Geophys. Res. 115, E06002. https://doi.org/10.1029/2009JE003485.
Baker, V.R., 1982. The Channels of Mars. Univ. of Tex. Press, Austin, TX.
Baker, V.R., 2001. Water and the martian landscape. Nature 412, 228–236.
Baker, V.R., 2009. The channeled scabland: a retrospective. Annu. Rev. Earth Planet Sci. 37, 393–411.
Baker, V.R., 2018. Long-term Hydrological Cycling on Early Mars. 49th Lunar and Planetary Science Conference. Abstract 1831.
Baker, V.R., Milton, D.J., 1974. Erosion by catastrophic floods on mars and Earth. Icarus 23, 27–41.
Baker, V.R., et al., 1991. Ancient oceans, ice sheets, and the hydrological cycle on Mars. Nature 352, 589–594.
Baker, V.R., Komatsu, G., Parker, T.J., Gulick, V.C., Kargel, J.S., Lewis, J.S., 1992. Channels and valleys on Venus: preliminary analysis of Magellan data. J. Geophys. Res. 97 (13), 421-13,444.
Baker, V.R., Komatsu, G., Gulick, V.C., Parker, T.J., 1997. Channels and valleys. In: Bougher, S.W., Hunten, D.M., Phillips, R.J. (Eds.), Venus II. Univ. of Ariz. Press, Tucson, AZ, pp. 757–793.
Barnes, S.J., 2006. In: Komatiite-hosted Nickel Sulfide Deposits: Geology, Geochemistry, and Genesis. Society of Economic Geologists, Special Publication 13, pp. 51–97.
Baumgartner, R.J., Fiorentini, M.L., Baratoux, D., Micklethwaite, S., Sener, A.K., Lorand, J.P., McCuaig, T.C., 2015. Magmatic controls on the genesis of Ni-Cu-(PGE) sulphide mineralisation on Mars. Ore Geol. Rev. 65, 400–412.
Baumgartner, R.J., Baratoux, D., Gaillard, F., Fiorentini, M.L., 2017. Numerical modeling of erosion and assimilation of sulfur-rich substrate by martian lava flows: implications for the genesis of massive sulfide mineralization on Mars. Icarus 296, 257–274.
Beaty, D.W., Clifford, S.M., Borg, L.E., Catling, D.C., Craddock, R.A., Des Merais, R.J., Farmer, J.D., Frey, H.V., Haberle, R.M., McKay, C.P., Newsom, H.E., Parker, T.J., Segura, T., Tanaka, K.L., 2005. Key science questions from the Second Conference on Early Mars: geologic, hydrologic, and climatic evolution and the implications for life. Astrobiology 5, 663–689.
Berman, D.C., Rodriguez, A.P., 2016. Evidence for magmatism as a trigger for catastrophic floods in Ravi Vallis. In: 47th Lunar and Planetary Science Conference. Abstract 2674.
Berman, D.C., Weitz, C.M., Rodriguez, A.P., Crown, D.A., 2017. Geologic mapping and spectral analyses of the source region of Shalbatana Vallis, Mars. Lunar and Planetary Science XLVIII. Abstract 1513.
Berman, D.C., Weitz, C.M., Rodriguez, A.P., Crown, D.A., 2018. Geologic map of the source region of Shalbatana Vallis. In: Mars. 49th Lunar and Planetary Science Conference. Abstract 1549.
Bibring, J.-P., Langevin, Y., Gendrin, A., Gondet, B., Poulet, F., Berthé, M., Soufflot, A., Arvidson, R., Mangold, N., Mustard, J., Drossart, P., OMEGA Team, 2005. Mars surface diversity as revealed by the OMEGA/Mars Express Observations. Science 307, 1576–1581.
Bibring, J.-P., Langevin, Y., Mustard, J.F., Poulet, F., Arvidson, R., Gendrin, A., Gondet, B., Mangold, N., Pinet, P., Forget, F., OMEGA Team, 2006. Global mineralogical and aqueous mars history derived from OMEGA/Mars Express data. Science 312, 400–404.
Bouley, S., Baratoux, D., Paulien, N., Missenard, Y., Saint-Bézar, B., 2018. The revised tectonic history of Tharsis. Earth Planet. Sci. Lett. 488, 126–133.
Bretz, J.H., 1969. The lake Missoula floods and the channeled scablands. J. Geol. 77, 505–543.
Breuer, D., Plesa, A.-C., Tosi, N., Grott, M., 2016. Water in the Martian interior – the geodynamical perspective. Meteoritics Planet Sci. 51 (11), 1959–1992. https://doi.org/10.1111/maps.12727.
Brustel, C., Flahaut, J., Hauber, E., Fueten, F., Quantin, C., Stesky, R., Davies, G.R., 2017. Valles Marineris tectonic and volcanic history inferred from dikes in eastern Coprates Chasma. J. Geophys. Res. 122, 1353–1371.
Burns, R.G., Fisher, D.S., 1990. Evolution of sulfide mineralization on Mars. J. Geophys. Res. 95, 14169–14173.
Burr, D.M., Parker, A.H., 2006. Gjotá Valles and implications for flood sediment deposition on Mars. Geophys. Res. Lett. 33, L22201. https://doi.org/10.1029/2006GL028011.
Byrne, P.K., Klimczak, C., Williams, D.A., Hurwitz, D.M., Solomon, S.C., Head, J.W., Preusker, F., Oberst, J., 2013. An assemblage of lava flow features on Mercury. J. Geophys. Res. 118, 1303–1322. https://doi.org/10.1002/jgre.20052.
Cabrol, N.A., 2018. The coevolution of life and environment on Mars: an ecosystem perspective on the robotic exploration of biosignatures. Astrobiology 18. https://doi.org/10.1089/ast.2017.1756.
Cabrol, N.A., Grin, E.A., Dawidowicz, G., 1997. A model of outflow generation by hydrothermal underpressure drainage in volcano-tectonic environment, Shalbatana Vallis (Mars). Icarus 125, 455–464.

Camp, V.E., Reidel, S.P., Ross, M.E., Brown, R.J., Self, S., 2017. Field-trip Guide to the Vents, Dikes, Stratigraphy, and Structure of the Columbia River Basalt Group, Eastern Oregon and Southeastern Washington. U.S. Geological Survey, Scientific Investigations. https://doi.org/10.3133/sir20175022N. Report 2017-5022-N.
Carling, P.A., Burr, D.M., Johnsen, T.F., Brennand, T.A., 2009. A review of open-channel megaflood depositional landforms on Earth and Mars. In: Burr, D.M., Carling, P.A., Baker, V.R. (Eds.), Megaflooding on Earth and Mars. Cambridge Univ. Press, Cambridge, pp. 33–49.
Carr, M.H., 1974. The role of lava erosion in the formation of lunar rilles and Martian channels. Icarus 22, 1–23.
Carr, M.H., 1979. Formation of Martian flood features by release of water from confined aquifers. J. Geophys. Res. 84, 2995–3007.
Carr, M.H., 1986. Mars: a water-rich planet? Icarus 68, 187–216.
Carr, M.H., 1995. The Martian drainage system and the origin of valley networks and fretted channels. J. Geophys. Res. 100, 7479–7507.
Carr, M.H., 1996. Water on Mars. Oxford University Press, New York, p. 229.
Carr, M.H., 2012. The fluvial history of Mars. Phil. Trans.: Mathematical, Physical and Engineering Sciences 370, 2193–2215.
Carr, M.H., Wänke, H., 1992. Earth and Mars: water inventories as clues to accretional histories. Icarus 98, 61–71.
Carr, M.H., Head III, J.W., 2003. Oceans on Mars: an assessment of the observational evidence and possible fate. J. Geophys. Res. 108, E5. https://doi.org/10.1029//2002JE0011963.
Carr, M.H., Head, J.W., 2010. Geologic history of mars. Earth Planet. Sci. Lett. 294, 185–203.
Carr, M.H., Head, J.W., 2015. Martian surface/near-surface water inventory: sources, sinks, and changes with time. Geophys. Res. Lett. https://doi.org/10.1002/2014GL062464.
Carr, M., Head, J.W., 2019. Mars: formation and fate of a frozen Hesperian ocean. Icarus 319, 433–443.
Carter, J., Poulet, F., Bibring, J.-P., Mangold, N., Murchie, S., 2013. Hydrous minerals on Mars as seen by CRISM and OMEGA imaging spectrometers: updated global view. J. Geophys. Res. 118, 831–858.
Cassanelli, J.P., Head, J.W., 2016. Lava heating and loading of ice sheets on early Mars: predictions for meltwater generation, groundwater recharge, and resulting landforms. Icarus 271, 237–264.
Cassanelli, J.P., Head, J.W., 2018a. Formation of outflow channels on Mars: testing the origin of Reull Vallis in Hesperia Planum by large-scale lava-ice interactions and topo-down melting. Icarus 305, 56–79.
Cassanelli, J.P., Head, J.W., 2018b. Large-scale lava-ice interactions on mars: investigating its role during late amazonian central Elysium plantia volcanism and the formation of Athabasca Valles. Planet. Space Sci. 158, 96–109.
Cataldo, V., Williams, D.A., Dundas, C.M., Keszthelyi, L.P., 2015. Limited role for thermal erosion by turbulent lava in proximal Athabasca Valles, Mars. J. Geophys. Res. 120, 1800–1819.
Chapman, M.G., Neukum, G., Dumke, A., Michael, G., van Gasselt, S., Kneissl, T., Zuschneid, W., Hauber, E., Ansan, V., Mangold, N., Masson, P., 2010a. Noachian-hesperian geologic history of the Echus Chasma and Kasei Valles system on mars: new data and interpretations. Earth Planet. Sci. Lett. 294, 256–271.
Chapman, M.G., Neukum, G., Dumke, A., Michael, G., van Gasselt, S., Kneissl, T., Zuschneid, W., Hauber, E., Mangold, N., 2010b. Amazonian geologic history of the Echus Chasma and Kasei Valles system on Mars: new data and interpretations. Earth Planet. Sci. Lett. 294, 238–255.
Chevrel, M.O., Baratoux, D., Hess, K.-U., Dingwell, D.B., 2014. Viscous flow behavior of tholeiitic and alkaline Fe-rich martian basalts. Geochem. Cosmochim. Acta 124, 348–365.
Christensen, P.R., et al., 2003. Morphology and composition of the surface of mars: mars odyssey THEMIS results. Science 300, 2056–2061.
Christensen, P.R., Bandfield, J.L., Rogers, A.D., Glotch, T.D., Hamilton, V.E., Ruff, S.W., Wyatt, M.B., 2008. Global mineralogy mapped from the mars global surveyor thermal Emission spectrometer. In: Bell, J. (Ed.), Chapter 9 in "The Martian Surface: Composition, Mineralogy, and Physical Properties". Cambridge University Press, New York, pp. 195–220.
Christensen, P.R., Fergason, R.L., 2013. THEMIS-derived thermal inertia mosaic of Mars: product description and science results. In: 44th Lunar and Planetary Science Conference, the Woodlands, TX. Abstract #2822.
Citron, R.I., Manga, M., Hemingway, D.J., 2018. Timing of oceans on Mars from shoreline deformation. Nature 555, 643–646.
Clifford, S.M., 1993. A model for the hydrologic and climatic behavior of water on Mars. J. Geophys. Res. 98 (10), 973-11,016.
Clifford, S.M., 2017. Insights and uncertainties regarding the existence, recharge, and extent of Martian groundwater flow based on the elevation and location of outflow channel activity. 19th EGU General Assembly. In: Proceedings from the Conference Held 23-28 April, 2017, in Vienna, Austria, p. 11431.
Clifford, S.M., Parker, T.J., 2001. The evolution of the Martian hydrosphere: implications for the fate of a primordial ocean and the current state of the northern plains. Icarus 154, 40–79.
Coffin, M.F., Eldholm, O., 1993. Scratching the surface: Estimating the dimensions of large igneous provinces. Geology 21, 515–518.
Coleman, N.M., 2003. Aqueous flows carved the outflow channels on Mars. J. Geophys. Res. 108 (E5), 5039. https://doi.org/10.1029/2002JE001940.
Coleman, N.M., 2005. Martian megaflood triggered chaos formation, revealing groundwater depth, cryosphere thickness, and crustal heat flux. J. Geophys. Res. 110, E12S20, 10.10292005JE002419.
Coleman, N.M., 2016. Secondary chaos on Mars produced substantial flooding. In: 47th Lunar and Planetary Science Conference. Abstract 1054.
Coleman, N.M., Baker, V.R., 2009. Surface morphology and origin of outflow channels in the Valles Marineris region. In: Burr, D.M., Carling, P.A., Baker, V.R. (Eds.), Chapter 9 in Megaflooding on Earth and Mars, pp. 172–193.
Cull-Hearth, S., Clark, M.C., 2017. A composite mineralogical map of Ganges Chasma and surroundings, Valles Marineris, mars. Planet. Space Sci. 142, 1–8.
Di Achille, G., Hynek, B.M., 2010. Ancient ocean on Mars supported by global distribution of deltas and valleys. Nat. Geosci. https://doi.org/10.1038/NGE0891.
Dohm, J.M., Ferris, J.C., Barlow, N.G., Baker, V.R., Mahaney, W.C., Anderson, R.C., Hare, T.M., 2004. The northwestern slope valleys (NSVs) region, Mars: a prime candidate site for the future exploration of Mars. Planet. Space Sci. 52, 189–198.
Dundas, C.M., Keszthelyi, L.P., 2014. Emplacement and erosive effects of lava in south Kasei Valles, Mars. J. Volcanol. Geoth. Res. 282, 92–102.
Dundas, C.M., McEwen, A.S., Diniega, S., Hansen, C.J., Byrne, S., McElwaine, J.N., 2017. The Formation of Gullies on Mars Today. Geological Society of London, Special Publications, 467. https://doi.org/10.1144/SP467.5.
Dundas, C.M., Cushing, G.E., Keszthelyi, L.P., 2019. The flood lavas of Kasei Valles, mars. Icarus 321, 346–357.
Durrant, L., Balme, M.R., Carling, P.A., Grindrod, P.M., 2017. Aqueous dune-like bedforms in Athabasca Valles and neighbouring locations utilized in palaeoflood reconstruction. Planet. Space Sci. 148, 45–55.
Edwards, C.S., Christensen, P.R., Hamilton, V.E., 2008. Evidence for extensive olivine-rich basalt bedrock outcrops in Ganges and Eos chasmas, Mars. J. Geophys. Res. 113, E11003 https://doi.org/10.1029/2008JE003091.
Ehlmann, B.L., 2014. The first billion years – warm and wet vs. cold and ice?. In: Eighth International Conference on Mars, Pasadena, CA Abstract 1245.
Ehlmann, B.L., Mustard, J.F., Murchie, S.L., Bibring, J.-P., Meunier, A., Fraeman, A.A., Langevin, Y., 2011. Subsurface water and clay mineral formation during the early history of Mars. Nature 479, 53–60.
Ernst, R.E., Buchan, K.L., 1997. Giant radiating dyke swarms: their use in identifying pre-Mesozoic large igneous provinces and mantle plumes. In: Mahoney, J.J., Coffin, M.F. (Eds.), Large Igneous Provinces. Geophysical Monograph 100. American Geophysical Union, Washington, DC, pp. 297–333.
Ernst, R.E., Buchan, K.L., 2003. Recognizing mantle plumes in the geological record. Annu. Rev. Earth Planet Sci. 31, 469–523.
Ernst, R.E., Buchan, K.L., Campbell, I.A., 2005. Frontiers in large igneous province research. Lithos 79, 271–297.
Fairén, A.G., Dohm, J.M., Baker, V.R., de Pablo, M.A., Ruiz, J., Ferris, J.C., Anderson, R.C., 2003. Episodic flood inundations of the northern plains of Mars. Icarus 165, 53–67.
Fairén, A.G., Schultze-Makuch, D., Rodriguez, A.P., Fink, W., Davila, A.F., Uceda, E.R., Furfaro, R., Amils, R., McKay, C.P., 2009. Evidence for Amazonian acidic liquid water on Mars – a reinterpretation of MER mission results. Planet. Space Sci. 57, 276–287.
Fairén, A.G., Davila, A.F., Gago-Duport, L., Haqq-Misra, J.D., Gil, C., McKay, C.P., Kasting, J.F., 2011. Cold glacial oceans would have inhibited phyllosilicate sedimentation on early Mars. Nat. Geosci. 4, 667–670.
Filiberto, J., Treiman, A.H., Le, L., 2008. Crystallization experiments on a Gusev Adirondack basalt composition. Meteoritics Planet Sci. 43, 1137–1146.
Garry, W.B., Bleacher, J.E., 2011. Emplacement scenarios for Vallis schoteri aristarchus plateau, the Moon. In: Ambrose, W.A., Williams, D.A. (Eds.), Recent Advances and Current Research Issues in Lunar Stratigraphy, vol. 477. Geological Society of America Special Paper, pp. 77–93. https://doi.org/10.1130/2011.2477(03.
Gellert, R., Rieder, R., Anderson, R.C., Brückner, J., Clark, B.C., Dreibus, G., Economou, T., Kingelhöfer, G., Lugmair, G.W., Ming, D.W., Squyres, S.W., d'Uston, C., Wänke, H., Yen, A., Zipfel, J., 2004. Chemistry of rocks and soils in gusev crater from the alpha particle X-ray spectrometer. Science 305, 829–832.
Ghatan, G.J., Zimbelman, J.R., 2006. Paucity of candidate coastal constructional landforms along proposed shorelines on Mars: implications for a northern lowlands-filling ocean. Icarus 185, 171–196.
Goetz, W., Bertelsen, P., Binau, C.S., Gunnlaugsson, H.P., Hviid, S.F., Kinch, K.M., Madsen, D.E., Madsen, M.B., Olsen, M., Gellert, R., Klingelhofer, G., Ming, D.W., Morris, R.V., Rieder, R., Rodionov, D.S., de Souza Jr., P.A., Schroder, C., Squyres, S.W., Wdowiak, T., Yen, A., 2005. Indication of drier periods on Mars from the chemistry and mineralogy of atmospheric dust. Nature 436, 62–65.
Gole, M.J., Robertson, J., Barnes, S.J., 2013. Extrusive origin and structural modification of the komatiitic Mount Keith ultramafic unit. Econ. Geol. 108, 1731–1752.
Gornitz, V., 1973. The origin of sinuous rilles. Moon 6, 337–356.
Goudge, T.A., Aureli, K.L., Head, J.W., Fassett, C.I., Mustard, J.F., 2015. Classification and analysis of candidate impact crater-hosted closed-basin lakes on Mars. Icarus 260, 346–367.
Greeley, R., 1971. Lunar hadley rille: considerations of its origin. Science 172, 722–725.
Greeley, R., Theilig, E., Guest, J.E., Carr, M.H., Masursky, H., Cutts, J.A., 1977. Geology of Chryse planitia. J. Geophys. Res. 82, 4093–4109.
Grove, T.L., Parman, S.W., 2004. Thermal evolution of the Earth as recorded by komatiites. Earth Planet. Sci. Lett. 219, 173–187.
Hall, J.L., Solomon, S.C., Head, J.W., 1986. Elysium region, Mars: tests of lithospheric loading models for the formation of tectonic features. J. Geophys. Res. 91, 11,377-11,392.
Hamilton, C.W., Mouginis-Mark, P.J., Sori, M.M., Scheidt, S.P., Bramson, A.M., 2018. Episodes of aqueous flooding and effusive volcanism associated with Hrad Vallis, Mars. J. Geophys. Res. https://doi.org/10.1029/2018JE005543.
Hand, E., 2012. Dreams of water on Mars evaporate. Nature 484, 153.
Head III, J.W., Crumpler, L.S., Aubele, J.C., Guest, J.E., Saunders, R.S., 1992. Venus volcanism: classification of volcanic features and structures, associations, and global distribution from Magellan data. J. Geophys. Res. 97, 13,153-13,197.
Head, J.W., Wilson, L., 1992. Lunar mare volcanism: stratigraphy, eruption conditions, and the evolution of secondary crust. Geochem. Cosmochim. Acta 56, 2155–2175.

Head III, J.W., Hiesinger, H., Ivanov, M.A., Kresslavsky, M.A., Pratt, S., Thomson, B.J., 1999. Possible ancient oceans on mars: evidence from mars orbiter laser altimeter data. Science 286, 2134–2137.
Head, J.W., Wilson, L., Mitchell, K.L., 2003. Generation of recent massive water floods at Cerberus Fossae, Mars by dike emplacement, cryospheric cracking, and confined aquifer groundwater release. Geophys. Res. Lett. 30, 1577. https://doi.org/10.1029//2003GL017135.
Head, J.W., Chapman, C.R., Strom, R.G., Fassett, C.I., Denevi, B.W., Blewett, D.T., Ernst, C.M., Watters, T.R., Solomon, S.C., Murchie, S.L., Prockter, L.M., Chabot, N.L., Gillis-Davis, J.J., Whitten, J.L., Goudge, T.A., Baker, D.M.H., Hurwitz, D.M., Ostrach, L.R., Xiao, Z., Merline, W.J., Kerber, L., Dickson, J.L., Oberst, J., Byrne, P.K., Klimczak, C., Nittler, L.R., 2011. Flood volcanism in the northern high latitudes of Mercury revealed by MESSENGER. Science 333, 1853–1856.
Head, J., Forget, F., Wordsworth, R., Turbet, M., Cassanelli, J., Palumbo, A., 2018. Two oceans on Mars?: history, problems, and prospects. In: 49th Lunar and Planetary Science Conference. Abstract 2194.
Hobbs, S.W., Pain, C.F., Clarke, J.D.A., 2011. Slope morphology of hills at the Mars Pathfinder landing site. Icarus 214, 258–264.
Hoefen, T.M., Clark, R.N., Bandfield, J.L., Smith, M.D., Pearl, J.C., Christensen, P.R., 2003. Discovery of olivine in the Nili Fossae region of mars. Science 302, 627–630.
Hopper, J.P., Leverington, D.W., 2014. Formation of Hrad Vallis (Mars) by low viscosity lava flows. Geomorphology 207, 96–113.
Houlé, M.G., Gibson, H.L., Lesher, C.M., Davis, P.C., Cas, R.A.F., Beresford, S.W., Arndt, N.T., 2008. Komatiitic sills and multigenerational peperite at Dundonald beach, abitibi greenstone belt, ontario: volcanic architecture and nickel sulfide distribution. Econ. Geol. 103, 1269–1284.
Houlé, M.G., Lesher, M., Davis, P.C., 2012. Thermomechanical erosion at the Alexo Mine, Abitibi greenstone belt, Ontario: implications for the genesis of komatiite-associated Ni-Cu-(PGE) mineralization. Miner. Deposita 47, 105–128.
Hulme, G., 1973. Turbulent lava flow and the formation of lunar sinuous rilles. Mod. Geol. 4, 107–117.
Hulme, G., 1974. The interpretation of lava flow morphology. Geophys. J. R. Astron. Soc. 39, 361–383.
Hulme, G., 1982. A review of lava flow processes related to the formation of lunar sinuous rilles. Geophys. Surv. 5, 245–279.
Hulme, G., Fielder, G., 1977. Effusion rates and rheology of lunar lavas. Philos. Trans. R. Soc. London, Ser. A 285, 227–234.
Huppert, H.E., Sparks, R.S.J., 1985. Cooling and contamination of mafic and ultramafic magmas during ascent through continental crust. Earth Planet. Sci. Lett. 74, 371–386.
Huppert, H.E., Sparks, R.S.J., Turner, J.S., Arndt, N.T., 1984. Emplacement and cooling of komatiite layers. Nature 309, 19–22.
Hurwitz, D.M., Fassett, C.I., Head, J.W., Wilson, L., 2010. Formation of an eroded lava channel within an Elysium Planitia impact crater: distinguishing between a mechanical and thermal origin. Icarus 210, 626–634.
Hurwitz, D.M., Head, J.W., Wilson, L., Hiesinger, H., 2012. Origin of lunar sinuous rilles: modeling effects of gravity, surface slope, and lava composition on erosion rates during the formation of Rima Prinz. J. Geophys. Res. 117, E00H14. https://doi.org/10.1029/2011JE004000.
Hurwitz, D.M., Head, J.W., Hiesinger, H., 2013a. Lunar sinuous rilles: distribution, characteristics, and implications for their origin. Planet. Space Sci. 79–80, 1–38.
Hurwitz, D.M., Head, J.W., Byrne, P.K., Xiao, Z., Solomon, S.C., Zuber, M.T., Smith, D.E., Neumann, G.A., 2013b. Investigating the origin of candidate lava channels on Mercury with MESSENGER data: theory and observations. J. Geophys. Res. 118, 471–486.
Ivanov, M.A., Head, J.W., 2001. Chryse Planitia, Mars: topographic configuration, outflow channel continuity and sequence, and tests for hypothesized ancient bodies of water using Mars Orbiter Laser Altimeter (MOLA) data. Journal of Geophysical Research 106, 3275–3295.
Jaeger, W.L., Keszthelyi, L.P., Skinner Jr., J.A., Milazzo, M.P., McEwen, A.S., Titus, T.N., Rosiek, M.R., Galuszka, D.M., Howington-Kraus, E., Kirk, R.L., HiRISE Team, 2010. Emplacement of the youngest flood lava on Mars: a short, turbulent story. Icarus 205, 230–243.
Jozwiak, L.M., Head, J.W., Zuber, M.T., Smith, D.E., Neumann, G.A., 2012. Lunar floor-fractured craters: classification, distribution, origin and implications for magmatism and shallow crustal structure. J. Geophys. Res. 117 https://doi.org/10.1029/2012JE004134.
Kargel, J.S., Komatsu, G., Baker, V.R., Strom, R.G., 1993. The volcanology of Venera and VEGA landing sites and the geochemistry of Venus. Icarus 103, 253–275.
Karlstrom, L., Richards, M., 2011. On the evolution of large ultramafic magma chambers and timescales for flood basalt eruptions. J. Geophys. Res. 116, B08216. https://doi.org/10.1029/2010JB008159.
Keszthelyi, L., Self, S., 1998. Some physical requirements for the emplacement of long basaltic lava flows. J. Geophys. Res. 103 (27), 447-27,464.
Keszthelyi, L., McEwen, A.S., Thordarson, T., 2000. Terrestrial analogs and thermal models for Martian flood lavas. J. Geophys. Res. 105 (15), 027-15,049.
Keszthelyi, L., Thordarson, T., McEwen, A., Haack, H., Guilbaud, M.-N., Self, S., Rossi, M.J., 2004. Icelandic analogs to Martian flood lavas. Geochem. Geophys. Geosyst. 5 https://doi.org/10.1029/2004GC0000758.
Keszthelyi, L., Self, S., Thordarson, T., 2006. Flood lavas on Earth, io and mars. J. Geol. Soc. London 163, 253–264.
Keszthelyi, L.P., Jaeger, W.L., Dundas, C.M., McEwen, A.S., 2014a. A new paradigm for, and questions about, volcanism on Mars. In: Eighth International Conference on Mars. Abstract 1189.
Keszthelyi, L., Jaeger, W., Dundas, M., Williams, D.A., Cataldo, V., 2014b. Evidence for possible mechanical erosion by lava at Athabasca Valles, Mars, from HiRISE and CTX images and topography. Lunar Planet. Sci. 45 abstract 1683.
Keszthelyi, L.P., Dundas, C.M., Jaeger, W.L., 2017. Is erosion by lava important on Mars?. In: GSA Annual Meeting in Seattle, Washington, USA paper No. 319-12.
Koeppen, W.C., Hamilton, V.E., 2008. Global distribution, composition, and abundance of olivine on the surface of Mars from thermal infrared data. J. Geophys. Res. 113, E05001 https://doi.org/10.1029/2007JE002984.
Komar, P.D., 1979. Comparisons of the hydraulics of water flows in Martian outflow channels with flows of similar scale on Earth. Icarus 37, 156–181.
Komar, P.D., 1980. Modes of sediment transport in channelized water flows with ramifications to the erosion of Martian outflow channels. Icarus 42, 317–329.
Komatsu, G., 2007. Rivers in the Solar System: water is not the only fluid flow on planetary bodies. Geography Compass 1, 480–502.
Komatsu, G., Baker, V.R., 1994. Meander properties of Venusian channels. Geology 22, 67–70.
Komatsu, G., Baker, V.R., Gulick, V.C., Parker, T.J., 1993. Venusian channels and valleys distribution and volcanological implications. Icarus 102, 1–25.
Korteniemi, J., Kukkonen, S., 2018. Volcanic structures within Niger and Dao Valles, Mars, and implications for ouflow channel evolution and Hellas basins rim development. Geophys. Res. Lett. 45, 2934–2944.
Kukkonen, S., Kostama, V.-P., 2018. Modification history of the Harmakhis Vallis outflow channel, Mars, based on CTX-scale photogeologic mapping and crater count dating. Icarus 299, 46–67.
Lapotre, M.G.A., Lamb, M.P., Williams, R.M.E., 2016. Canyon formation constraints on the discharge of catastrophic outburst floods of Earth and Mars. J. Geophys. Res. 121, 1232–1263.
Larsen, I.J., Lamb, M.P., 2016. Progressive incision of the Channeled Scablands by outburst floods. Nature 538, 229–232.
Leask, H.J., Wilson, L., Mitchell, K.L., 2006a. formation of Aromatum chaos, mars: morphological development as a result of volcano-ice interactions. J. Geophys. Res. 111, E08071 https://doi.org/10.1029/2005JE002549.
Leask, H.J., Wilson, L., Mitchell, K.L., 2006b. Formation of Ravi Vallis outflow channel, Mars: morphological development, water discharge, and duration estimates. J. Geophys. Res. 111, E08070 https://doi.org/10.1029/2005JE002550.
Leask, H.J., Wilson, L., Mitchell, K.L., 2007. Formation of Mangala Valles outflow channel, mars: morphological development, water discharge, and duration estimates. J. Geophys. Res. 112, E08003 https://doi.org/10.1029/2006JE002851.
Leone, G., 2014. A network of lava tubes as the origin of labyrinthus Noctis and Valles Marineris on mars. J. Volcanol. Geoth. Res. 277, 1–8.
Leone, G., 2017. Mangala Valles, Mars: a reassessment of formation processes based on a new geomorphological and stratigraphic analysis of the geological units. J. Volcanol. Geoth. Res. 337, 62–80.
Leone, G., 2018. Comments to "A composite mineralogical map of Ganges Chasma and surroundings, Valles Marineris, mars" by selby cull-hearth and M. Caroline Clark (planetary and Space science 142. Planet. Space Sci. 1–8. https://doi.org/10.1016/j.pss.2018.08.002.
Lesher, C.M., 2017. Roles of xenomelts, xenoliths, xenocrysts, xenovolatiles, residues, and skarns in the genesis, transport, and localization of magmatic Fe-Ni-Cu-PGE sulfides and chromite. Ore Geol. Rev. 90, 465–484.
Lesher, C.M., Campbell, I.H., 1993. Geochemical and fluid dynamic modeling of compositional variations in Archean komatiite-hosted nickel sulfide ores in Western Australia. Econ. Geol. 88, 804–816.
Leverington, D.W., 2004. Volcanic rilles, streamlined islands, and the origin of outflow channels on Mars. J. Geophys. Res. 109, E10011 https://doi.org/10.1029/2004JE002311.
Leverington, D.W., 2005. Evaluation of candidate crater-lake sites on Mars. In: 36th Lunar and Planetary Science Conference. Abstract 1522.
Leverington, D.W., 2006. Volcanic processes as alternative mechanisms of landform development at a candidate crater-lake site near Tyrrhena Patera, Mars. J. Geophys. Res. 111, E11002 https://doi.org/10.1029/2004JE002382.
Leverington, D.W., 2007. Was the Mangala Valles system incised by volcanic flows? J. Geophys. Res. 112, E11005 https://doi.org/10.1029/2007JE002896.
Leverington, D.W., 2009. Reconciling channel formation mechanisms with the nature of elevated outflow systems at Ophir and Aurorae Plana, Mars. J. Geophys. Res. 114, E10005 https://doi.org/10.1029/2009JE003398.
Leverington, D.W., 2011. A volcanic origin for the outflow channels of Mars: key evidence and major implications. Geomorphology 132, 51–75.
Leverington, D.W., 2014. Did large volcanic channel systems develop on Earth during the Hadean and Archean? Precambrian Res. 246, 226–239.
Leverington, D.W., 2018. Is Kasei Valles (Mars) the largest volcanic channel in the solar system? Icarus 301, 37–57.
Leverington, D.W., Mann, J.D., Teller, J.T., 2000. Changes in the bathymetry and volume of glacial Lake Agassiz between 11,000 and 9300 ^{14}C yr B.P. Quat. Res. 54, 174–181.
Leverington, D.W., Mann, J.D., Teller, J.T., 2002. Changes in the bathymetry and volume of glacial Lake Agassiz between 9200 and 7600 ^{14}C yr B.P. Quat. Res. 57, 244–252.
Leverington, D.W., Maxwell, T.A., 2004. An igneous origin for features of a candidate crater-lake system in western Memnonia, Mars. J. Geophys. Res. 109, E06006 https://doi.org/10.1029//2004JE002237.
Levy, J.S., Head, J.W., 2005. Evidence for remnants of ancient ice-rich deposits: Mangala Valles outflow channel, Mars. Terra. Nova 17, 503–509.
Maaløe, S., 2002. Physical behavior of the plume source during intermittent eruptions of Hawaiian basalts. Contrib. Mineral. Petrol. 142, 653–665.
Malin, M.C., Edgett, K.S., 1999. Oceans or seas in the Martian northern lowlands: high resolution imaging tets of proposed coastlines. Geophys. Res. Lett. 26 (19), 3049–3052.
Mangold, N., Ansan, V., Baratoux, D., Costard, F., Dupeyrat, L., Hiesinger, H., Masson, Ph, Neukum, G., Pinet, P., 2008. Identification of a new outflow channel on Mars in Syrtis Major Planum using HRSC/MEx data. Planet. Space Sci. 56, 1030–1042.

Mangold, N., Loizeau, D., Poulet, F., Ansan, V., Baratoux, D., LeMouelic, S., Bardintzeff, J.M., Platevoet, B., Toplis, M., Pinet, P., Masson, Ph, Bibring, J.P., Gondet, B., Langevin, Y., Neukum, G., 2010. Mineralogy of recent volcanic plains in the Tharsis region, Mars, and implications for platy-ridged flow composition. Earth Planet. Sci. Lett. 294, 440–450.

Mangold, N., Baratoux, D., Witasse, O., Encrenaz, T., Sotin, C., 2016. Mars: a small terrestrial planet. Astron. AstroPhys. Rev. 24, 15. https://doi.org/10.1007/s00159-016-0099-5.

Mars Channel Working Group, 1983. Channels and valleys on mars. Geol. Soc. Am. Bull. 94, 1035–1054.

Masursky, H., Boyce, J.M., Dial, A.L., Schaber, G.G., Strobell, M.E., 1977. Classification and time of formation of Martian channels based on Viking data. J. Geophys. Res. 82, 4016–4038.

Max, M.D., Clifford, S.M., 2001. Initiation of Martian outflow channels: related to the dissociation of gas hydrate? Geophys. Res. Lett. 28, 1787–1790.

Marra, W.A., Hauber, E., McLelland, S., Murphy, B., Parsons, D.R., Conway, S.J., Roda, M., Govers, R., Kleinhans, M.G., 2014. Pressurized groundwater outflow experiments and numerical modeling for outflow channels on Mars. J. Geophys. Res. 119, 2668–2693. https://doi.org/10.1002/2014JE004701.

McGovern, P.J., Solomon, S.C., Smith, D.E., Zuber, M.T., Simons, M., Wieczorek, M.A., Phillips, R.J., Neumann, G.A., Aharonson, O., Head, J.W., 2002. Localized gravity/topography admittance and correlation spectra on Mars: implications for regional and global evolution. J. Geophys. Res. 107, 5136. https://doi.org/10.1029/2002JE001854.

McKay, C.P., 1992. Mars: A Reassessment of its Interest to Biology. Exobiology in Solar System Exploration. NASA Ames Research Center, Moffet Field, CA, United States, pp. 67–82.

McLennan, S.M., 2012. Geochemistry of sedimentary processes on Mars. In: Sedimentary Geology of Mars. SEPM Special Publication No. 102, Society for Sedimentary Geology, pp. 119–138.

Meresse, S., Costard, F., Mangold, N., Masson, P., Neukum, G., the HRSC Co-I Team, 2007. Formation and evolution of the chaotic terrains by subsidence and magmatism: Hydraotes Chaos, Mars. Icarus 194, 487–500.

Milton, D.J., 1973. Water and processes of degradation in the Martian landscape. J. Geophys. Res. 78, 4037–4047.

Moore, J.M., Clow, G.D., Davis, W.L., Gulick, V.C., Janke, D.R., McKay, C.P., Stoker, C.R., Zent, A.P., 1995. The circum-Chryse region as a possible example of a hydrologic cycle on Mars: geologic observations and theoretical evaluation. J. Geophys. Res. 100, 5433–5447.

Mouginot, J., Pommerol, A., Beck, P., Kofman, W., Clifford, S.M., 2012. Dielectric map of the Martian northern hemisphere and the nature of plain filling materials. Geophys. Res. Lett. 39, L02202. https://doi.org/10.1029/2011GL050286.

Murase, T., McBirney, A.R., 1970. Viscosity of lunar lavas. Science 167, 1491–1493.

Murase, T., McBirney, A.R., 1973. Properties of some common igneous rocks and their melts at high temperatures. Bull. Geol. Soc. Am. 84, 3563–3592.

Nelson, D.M., Greeley, R., 1999. Geology of Xanthe Terra outflow channels and the mars pathfinder landing site. J. Geophys. Res. 104, 8653–8669.

Neumann, G.A., Zuber, M.T., Wieczorek, M.A., McGovern, P.J., Lemoine, F.G., Smith, D.E., 2004. Crustal structure of Mars from gravity and topography. J. Geophys. Res. 109, E08002 https://doi.org/10.1029/2004JE002262.

Nisbet, E.G., Cheadle, M.J., Arndt, N.T., Bickle, M.J., 1993. Constraining the potential temperature of the Archean mantle: a review of the evidence from komatiites. Lithos 30, 291–307.

Nummedal, D., Prior, D.B., 1981. Generation of Martian chaos and channels by debris flows. Icarus 45, 77–86.

Ori, G.G., Mosangini, C., 1998. Complex depositional systems in Hydraotes Chaos, Mars: an example of sedimentary process interactions in the Martian hydrological cycle. J. Geophys. Res. 103 (22), 713–722, 723.

Pan, L., Ehlmann, B.L., Carter, J., Ernst, C., 2017. The stratigraphy and history of Mars' northern lowlands through mineralogy of impact craters: a comprehensive survey. J. Geophys. Res. 122, 1824–1854.

Parker, T.J., Gorsline, D.S., Saunders, R.S., Pieri, D.C., Schneeberger, D.M., 1993. Coastal geomorphology of the Marrtian northern plains. J. Geophys. Res. 98 e6, 11,061-11,078.

Plescia, J.B., 1990. Recent flood lavas in the Elysium region of Mars. Icarus 88, 465–490.

Pretlow, R.W., 2013. A Geomorphological Investigation of Paleoshorelines on Mars. A Report Prepared in Partial Fulfillment of the Requirements for the Degree of Master of Science. University of Washington, Seattle, Washington.

Putzig, N.E., Mellon, M.T., 2007. Apparent thermal inertia and the surface heterogeneity of Mars. Icarus 191, 68–94.

Rapin, W., et al., 2018. In situ analysis of opal in Gale crater, Mars. J. Geophys. Res. 123 https://doi.org/10.1029/2017JE005483.

Reidel, S.P., 1998. Emplacement of Columbia River flood basalt. J. Geophys. Res. 103 (27), 393-27,410.

Rice, J.W., Baker, V.R., 2015. New observations of Martian outflow channel flood deposits. In: 46th Lunar and Planetary Science Conference, Houston abstract 2979.

Roberts, C.E., Gregg, T.K.P., 2018. Rima Marius, the Moon: formation of lunar sinuous rilles by constructional and erosional processes. Icarus. https://doi.org/10.1016/j.icarus.2018.02.033.

Rodriguez, J.A.P., Sasaki, S., Miyamoto, H., 2003. Nature and hydrological relevance of the Shalbatana complex underground cavernous system. Geophys. Res. Lett. 30 https://doi.org/10.1029/2002GL016547.

Rogers, A.D., Christensen, P.R., Bandfield, J.L., 2005. Compositional heterogeneity of the ancient Martian crust: analysis of Ares Vallis bedrock with THEMIS and TES data. J. Geophys. Res. 110, E05010 https://doi.org/10.1029/2005JE002399.

Rodriguez, J.A.P., Kargel, J.S., Tanaka, K.L., Crown, D.A., Berman, D.C., Fairén, A.G., Baker, V.R., Furfaro, R., Candelaria, P., Sasaki, S., 2011. Secondary chaotic terrain formation in the higher outflow channels of southern circum-Chryse, Mars. Icarus 213, 150–194.

Rodriguez, J.A.P., Bourke, M., Tanaka, K.L., Miyamoto, H., Kargel, J., Baker, V., Fairén, A.G., Davies, R.J., Bridget, L., Santiago, R.L., Hernández, M.Z., Berman, D.C., 2012. Infiltration of Martian outflow channel floodwaters into lowland cavernous systems. Geophys. Res. Lett. 39, L22201. https://doi.org/10.1029/2012GL053225.

Rodriguez, J.A.P., Fairén, A.G., Tanaka, K.L., Zarroca, M., Linares, R., Platz, T., Komatsu, G., Miyamoto, H., Kargel, J.S., Yan, J., Gulick, V., Higuchi, K., Baker, V.R., Glines, N., 2016. Tsunami waves extensively resurfaced the shorelines of an early Martian ocean. Sci. Rep. 6 https://doi.org/10.1038/srep25106. Article 25106.

Sagan, C., Toon, O.B., Gierasch, P.J., 1973. Climatic change on mars. Science 181, 1045–1049.

Salvatore, M.R., Mustard, J.F., Head III, J.W., Rogers, A.D., Cooper, R.F., 2014. The dominance of cold and dry alteration processes on recent Mars, as revealed through pan-spectral orbital analyses. Earth Planet. Sci. Lett. 404, 261–272.

Sato, H., Kurita, K., Baratoux, D., 2010. The formation of floor-fractured craters in Xanthe Terra. Icarus 207, 248–264.

Schonfeld, E., 1977a. Martian volcanism. In: Lunar Sci. Conf, 8th. Houston, Lunar and Planetary Institute, Houston, TX, pp. 843–845 (abstract).

Schonfeld, E., 1977b. Volcanism on Mars and the Moon. Abstracts of Papers Presented at the Planetary Sciences Division Meeting, vol. 9. Bulletin of the American Astronomical Society, Honalulu, Hawaii, p. 453 abstract 034-PT.

Schonfeld, E., 1979. Origin of Valles Marineris. In: 10th Proceedings of the Lunar Science Conference. Lunar and Planetary Institute, Houston, Houston, TX, pp. 3031–3038.

Schulze-Makuch, D., Dohm, J.M., Fan, C., Fairén, A.G., Rodriguez, J.A.P., Baker, V.R., Fink, W., 2007. Exploration of hydrothermal targets on Mars. Icarus 189, 308–324.

Scott, D.H., Tanaka, K.L., 1986. Geologic map of the western equatorial region of Mars. U.S. Geol. Surv. Geol. Invest. Ser. Map I-1802-A.

Sewell, K.S., Hughes, C.G., Graettinger, A.H., 2017. Qualifying Martian maars using CTX imagery. Lunar and Planetary Science XLVIII. Abstract 1349.

Sharp, R.P., 1973. Mars: fretted and chaotic terrains. J. Geophys. Res. 78, 4073–4083.

Sharp, R.P., Malin, M.C., 1975. Channels on mars. Bull. Geol. Soc. Am. 86, 593–609.

Sklar, L., Dietrich, W.E., 1998. River longitudinal profiles and bedrock incision models: stream power and the influence of sediment supply. In: Tinkler, K.J., Wohl, E.E. (Eds.), Rivers over Rock: Fluvial Processes in Bedrock Channels, vol. 107. American Geophysical Union, Washington, DC. https://doi.org/10.1029/GM107p0237.

Smith, D., Neumann, G., Arvidson, R.E., Guinness, E.A., Slavney, S., 2003. Mars Global Surveyor Laser Altimeter Mission Experiment Gridded Data Record. NASA Planetary Data System, Greenbelt, MD., MOLA Gridded Data Record, MGS-M-MOLA-MEGDR-L3-V1.0.

Squyres, S.W., 1989. Urey prize lecture: water on mars. Icarus 79, 229–288.

Squyres, S.W., et al., 2004. The Sprit rover's Athena science investigation at Gusev crater, Mars. Science 305, 794–799.

Staude, S., Barnes, S.J., Le Vaillant, M., 2016. Evidence of lateral thermomechanical erosion of basalt by Fe-Ni-Cu sulfide melt at Kambalda, Western Australia. Geology 44, 1047–1050.

Staude, S., Barnes, S.J., Le Vaillant, 2017. Thermomechanical erosion of ore-hosting embayments beneath komatiite lava channels: textural evidence from Kambalda, Western Australia. Ore Geol. Rev. 90, 446–464.

Stockstill-Cahill, K.R., McCoy, T.J., Nittler, L.R., Weider, S.Z., Hauck, I.I.S.A., 2012. Magnesium-rich crustal compositions on Mercury: implications for magmatism from petrologic modeling. J. Geophys. Res. 117, E00L15. https://doi.org/10.1029/2012JE004140.

Tanaka, K.L., 1997. Sedimentary history and mass flow structures of Chryse and acidalia planitia, mars. J. Geophys. Res. 102, 4131–4149.

Thordarson, T., Self, S., 1993. The Laki (skaftar Fires) and grimsvotn eruptions, 1783-1785. Bull. Volcanol. 55, 233–263.

Toon, O.B., Pollack, J.B., Ward, W., Burns, J.A., Bilski, K., 1980. The astronomical theory of climatic change on mars. Icarus 44, 552–607.

Tosca, N.J., Knoll, A.H., 2009. Juvenile chemical sediments and the long-term persistence of water at the surface of Mars. Earth Planet. Sci. Lett. 286, 379–386.

Voelker, M., Hauber, E., Stephan, K., Jaumann, R., 2018. Volcanic flows versus water- and ice-related outburst deposits in eastern Hellas: a comparison. Icarus 307, 1–16.

Wänke, H., Dreibus, G., 1994. Chemistry and accretion history of Mars. Phil. Trans. Roy. Soc. Lond.: Phys. Sci. Eng. 349, 285–293.

Warner, N., Gupta, S., Kim, J.-R., Lin, S.-Y., Muller, J.-P., 2010. Hesperian equatorial thermokarst lakes in Ares Vallis as evidence for transient warm conditions on Mars. Geology 38, 71–74.

Weill, D.F., Grieve, R.A., McCallum, I.S., Bottinga, Y., 1971. Mineralogy-petrology of lunar samples. Microprobe studies of samples 12021 and 12022; viscosity of melts of selected lunar compositions. In: Proceedings of the Second Lunar Science Conference, vol. 1. The M.I.T. Press, pp. 413–430.

Wilhelms, D., 1987. The geologic history of the Moon. U. S. Geol. Surv. Prof. Pap. 1348, Washington, DC.

Williams, D.A., Kerr, R.C., Lesher, C.M., 1998. Emplacement and erosion by Archean komatiite lava flows at Kambalda: revisited. J. Geophys. Res. 103, 27533–27549.

Williams, D.A., Fagents, S.A., Greeley, R., 2000. A reassessment of the emplacement and erosional potential of turbulent, low-viscosity lavas on the Moon. J. Geophys. Res. 105, 20189–20205. https://doi.org/10.1029/1999JE001220.

Williams, D.A., Kerr, R.C., Lesher, M., Barnes, S.J., 2001. Analytical/numerical modeling of lava emplacement and thermal erosion at Perseverance, Western Australia. J. Volcanol. Geoth. Res. 110, 27–55.

Williams, D.A., Greeley, R., Hauber, E., Gwinner, K., Neukum, G., 2005. Erosion by flowing martian lava: new insights for hecates tholus from mars Express and MER data. J. Geophys. Res. 110, E05006 https://doi.org/10.1029/2004JE002377.

Williams, D.A., Kerr, R.C., Lesher, C., 2011. Mathematical modeling of thermomechanical erosion beneath Proterozoic komatiitic basaltic sinuous rilles in the Cape Smith Belt, New Quebec, Canada. Miner. Deposita. https://doi.org/10.1007/s00126-011-0364-5.

Wilson, J.H., Mustard, J.F., 2013. Exposures of olivine-rich rocks in the vicinity of ares Vallis: implications for Noachian and hesperian volcanism. J. Geophys. Res. 118, 916–929.

Wilson, L., Head, J.W., 2002. Tharsis-radial graben systems as the surface manifestation of plume-related dike intrusion complexes: models and implications. J. Geophys. Res. 107, 5057, 10.10292001JE001593.

Wilson, L., Head, J.W., 2017a. Generation, ascent and eruption of magma on the Moon: new insights into source depths, magma supply, intrusions and effusive/explosive eruptions (Part 1: theory). Icarus 283, 146–175.

Wilson, L., Head, J.W., 2017b. Generation, ascent and eruption of magma on the Moon: new insights into source depths, magma supply, intrusions and effusive/explosive eruptions (Part 2: predicted emplacement processes and observations). Icarus 283, 176–223.

Wilson, L., Head, J.W., 2018. Lunar floor-fractured craters: modes of dike and sill emplacement and implications of gas production and intrusion cooling on surface morphology and structure. Icarus 305, 105–122.

Wilson, L., Ghatan, G.J., Head III, J.W., Mitchell, K.L., 2004. Mars outflow channels: a reappraisal of the estimation of water flow velocities from water depths, regional slopes, and channel floor properties. J. Geophys. Res. 109, E09003 https://doi.org/10.1029/2004JE002281.

Wilson, L., Bargery, A.S., Burr, D.M., 2009a. Dynamics of fluid flow in Martian outflow channels. In: Burr, D.M., Carling, P.A., Baker, V.R. (Eds.), Chapter 16 in Megaflooding on Earth and Mars, pp. 290–311.

Wilson, L., Mouginis-Mark, P.J., Tyson, S., Mackown, J., Garbeil, H., 2009b. Fissure eruptions in Tharsis, Mars: implications for eruption conditions and magma sources. J. Volcanol. Geoth. Res. 185, 28–46.

Wordsworth, R.D., 2016. The climate of early Mars. Annu. Rev. Earth Planet Sci. 44, 381–408.

Zuber, M.T., 2018. Oceans on Mars formed early. Nature 555, 590–591.